# A COMPARATIVE STUDY OF FOUR UCAV WING LAYOUTS – HIGH SPEED AERO PERFORMANCE & STABILITY CONSIDERATIONS

*Dr. R. K. Nangia* *Dr. M. E. Palmer*

Nangia Aero Research Associates,
WestPoint, 78-Queens Road, BRISTOL, BS8 1QX, UK.
Tel: +44 (0)117-987 3995 Fax: +44 (0)117-987 3995

**Keywords**: *Wing-Design, UCAV, Joined-Wings, Aero-Performance*

## Abstract

*Currently there is a revival of interest in flying wings and unconventional layouts for military (and civil) use. The military context has arisen from the future "stealthy" HALE and UCAV aircraft. Many other "advanced" aircraft concepts e.g. Joined-Wing arrangements are being studied on the premise of structural advantages. For evaluation, questions on aerodynamics, control and structural efficiency arise. Compared with conventional wing / tail arrangements, the unconventional layouts have a special set of very different constraints. These are mentioned.*

*On layouts without a trim surface, the constraints on the wing pitching moment dictate the design camber and twist. Control power requirements can be high because of effectively short moment arms. The camber and twist are strongly dependent on trim stability margins. This aspect needs to be included in detail when comparing with the more unconventional layouts e.g. joined wing with a wider choice of control locations.*

*This paper is concerned with the study of four wing layouts for UCAV applications. It is inspired in part by the need to understand a variety of wings (in public domain) that are, at first sight, aimed at similar missions. A second reason is to see if the HALE type joined wing can also be developed into the UCAV role.*

*It is shown that, starting from basic information such as the planform, we are able to predict the anticipated performance with sufficient confidence for comparative assessments. The joined wing layout could provide an attractive option for UCAV's. With more detailed studies it may be possible to develop it for multi-roles incorporating some of the HALE (Sensorcraft) functions. Further work is proposed in several areas.*



## 1 INTRODUCTION & BACKGROUND

There is a revival of interest in flying wings and unconventional layouts for military (and civil) use. Taking the military flying wings first, **Fig.1**, there are requirements for "stealthy" High Altitude Long Endurance (HALE) and Unmanned Combat Air Vehicle (UCAV) type aircraft. The Northrop B-2 aircraft has been a recent fore-runner of the technologies. The civilian interest has been "sparked" from US studies on a large Blended Wing Body (BWB) aircraft, Refs.1-2. Many other "advanced" aircraft concepts e.g. Joined-Wing arrangements, **Fig.2**, are being studied. **Fig.3** alludes to a series of structural advantages claimed for such layouts (Refs.3-4).

Questions arise on aerodynamic, control and structural efficiency, Refs.5-8. Compared with conventional wing / tail arrangements, flying wings have a very different and specific set of constraints e.g. in the military context:

- "Stealth" considerations restrict the wing span and aspect ratio.
- The blended configuration has high planform taper and multiple planform cranks over Leading (LE) or Trailing edges (TE).
- The thickness to chord ratio (t/c) on the center-section needs to be large to accommodate weapons bays, powerplant.
- The flying wing planform results in small moment arms (longitudinal).

There are, of course, many other constraints as mentioned in Ref.2. A detailed understanding of stability margins is required when comparing different planforms.

On Joined wing layouts, several questions arise and some of these have been addressed

with respect to HALE Sensorcraft configurations in Refs.9-15. Very high AR can be achieved at the expense of strength and structural rigidity issues.

### This Paper

We take a comparative look at a series of flying wing UCAV's (Ref.16) and a joined wing UCAV (Ref.17) that owes its origin to HALE concepts (Ref.15). The emphasis will be on high speed performance with a "reasonable" level of design sophistication (appropriate camber and twist and stability levels). Usually, cruise $C_L$ will be lower than for conventional aircraft. The wing-tips do however operate at high local lift (highly tapered). Similarly, field performance becomes challenging. The low speed work (including controls) is deferred to another paper.

We need to be aware of the different flow solvers and their limitations when dealing with "unusual" types. To further the understanding with a quick "turn-around" whilst considering several layouts, it has been necessary to develop a strategy using "appropriate" solvers.

## 2. GEOMETRY VARIATIONS, MODELLING & PROCESS

We look at various planforms that may be applicable to the UCAV role. These include a series of flying wings and a joined wing configuration. The design process utilises various methods and solvers (linear theory, panel method and Euler) and can include Inverse techniques as required. The mission flight envelopes can be derived. The aerodynamics of planar and designed configurations can then be assessed and related to the performance criteria.

### 2.1 Flying Wings UCAV's, Geometry Choice

Several layouts, as for the X-45A, X-45C and the X-47B, are feasible, **Fig.4**. Concerning Take-Off weight (TOW) and endurance figures, different values are apparent from different sources (e.g. journals: Flight International, Unmanned Vehicles). For the small developmental X-45A the TOW is between 12,000 and 15,000 lb with an endurance of between 90 minutes and 3 hours. For the X-45C, TOW is of the order of 36,500lb with a range of 2600nm. For the X-47B, TOW is approximately 42,000 lb and a range 3000 nm.

Based on the X-series of UCAV (public domain), **Fig.5** shows typical layouts, U1, U2 and U3. It is easier to visualise the geometry non-dimensionalised in terms of semi-span (s =1). The planforms comprise three spanwise regions: the inner wing (centre-line to first crank, thickened to house power-plant and payload), the outer wing and the tip (tapers to zero chord). For this initial study we have set aerofoil thickness at 7% t/c. As the design process develops, aerofoils can be adapted (cambered) to suit specific requirements. LE and TE devices can be employed to tailor lift for take-off and landing. Planform-U1 (Aspect Ratio AR 3.230) is based on the experimental aircraft X-45A. The LE sweep is constant from centreline to tip at about 43°. The planform features an elongated forward central fuselage strake area and a constant chord outer wing. The TE is cranked ±43° at y/s=0.4 and 0.8. Note the possible variations of cranks and also the location of the half-chord sweep lines. Planform-U2 (AR 3.198) is based on the X-45C. It resembles a delta wing with LE sweep of 54°. The TE is cranked ±26° at y/s=0.3 and 0.85. The X-47B has inboard LE sweep of 54° (note X-45C) with 30° LE sweep outboard. The TE is cranked ±30° at y/s=0.45 and 0.75. The U3 planform (AR 5.094) is based on the X-47B but with the inboard LE sweep increased to 60°. The TE is cranked ±30° at y/s=0.4 and 0.8 providing a constant chord outer wing.

Possible $C_L$ and Altitude variations with Mach number within the flight design envelope are shown in **Fig.6**. These give an idea of the Mach - $C_L$ requirements, wing area, Reynolds number etc. Subsonic performance is limited by altitude and $C_L$ available within suitable stability constraints. The transonic design point is near $C_L = 0.2$ at Mach 0.8+. On conventional aircraft, the equivalent design point is at $C_L$ near 0.5 at Mach 0.8+.

### 2.2 Joined-Wing Layout

**Fig.7** shows the outline of the UCAV derived from the High Altitude Long Endurance UAV

configurations (Refs.15 & 17). We have taken the Lambda joined-wing planform and developed the concept for flight at Mach 0.8. This cruise condition may be more suited to the UCAV role for an aircraft with a cruise weight of 50,000lb. Typical cruise $C_L$ may lie between 0.2 and 0.4 with t/c = 7%. The LJAST planform has AR= 10.94 based on the front and tip wing areas (shaded). Total planform area gives AR=8.15. The Mach number, altitude, $C_L$ and wing loading (W/S) relationships are shown in **Fig.8**. Note that $C_L$ is usually based on the total front wing area but scales for $C_L$ and W/S based on both front wing and total wing areas are shown. The rear-wing has an area 70% of the front-wing. The design $C_L$=0.4 sizes the UCAV with span near 88ft, wing area (front) close to 710ft$^2$. Assuming TOW = 55,000lb, at Mach 0.2, $C_L$ near 1.3 would be required (Re= 1.42x10$^6$/ft), whilst landing at Mach 0.15 (Re= 1.07x10$^6$/ft) requires $C_L$ of 1.2. It is interesting to reflect that on conventional aircraft, the cruise $C_L$ values are near 0.5 and take-off / landing $C_L$ values near 0.8 to 1.2.

### 2.3 Modelling Techniques & Process

The analysis presented here is aimed at early design assessment, rather than "fine- tuning" or refining an already "reasonable" layout. In the early design phase, one needs to conduct a "wide" range of parametric studies and a fast turn-around is required with good reliability. At this stage, the aim is not for a "hands-off" approach as it is extremely important to understand and interact with the various features – aerodynamics, geometry and methods.

Various methods are available: linear surface (with and without attained thrust), panel method (also, with and without attained thrust), Euler Solver, and Inverse techniques, e.g. Refs.18-21. The Euler solvers imply higher computer usage, hours compared with seconds / minutes for the linear or panel solvers.

Experience with several different types of configurations (e.g. Refs.22-35) suggests that attained thrust methods generally lead to more realistic and practically achievable spanwise lift loadings rather than purely minimum drag methods with near-elliptic lift loadings. The latter implies very high local lift at the tip on highly tapered wings (aft-swept).

Based on past experience of designing transonic cruise wings, the strategy is to "partition" the design problem and use appropriate solvers for the different aspects before combining and evaluating. For aerofoil thickness design (at low $C_L$), Panel and Euler methods are used together with inverse techniques. This enables an idea of Wave-drag contribution as well as arriving at "good" pressure distributions, shock location, and maximising t/c. The wing sweep has a strong effect. Skin friction terms are derived as per simpler estimation methods (Refs.36-37) or data sheets (traditional manner). Camber and twist design is via linear theory or panel code with attained thrust. A series of modes are used to develop camber and twist. This is justified in view of the low design $C_L$ and low local supersonic Mach numbers. In this early analysis, the modes extend over the whole of the planform. The method, however, permits choice of other modes that allow certain portions of the planform to be omitted from the design, e.g. the central area housing the propulsion system. In this paper, the main emphasis is on the camber design of the whole planform.

The camber and twist terms are then combined to yield a configuration that is evaluated with Panel and Euler solvers. Viscous (boundary layer effects) can be introduced at this stage. Inverse techniques can be in action next for refinements as necessary. In general, for low speed, subsonic, evaluations, the Euler methods are not really called for.

We will consider the possible flight envelopes and then take each planform in turn (planar and designed cases) before presenting selected comparisons and performance criteria.

## 3. LAYOUT - U1

As mentioned earlier, the emphasis is on appreciation of camber and twist derivation. We have chosen to design camber etc. for Mach 0.8 cruise, $C_L$ = 0.2 with the required levels of longitudinal stability. First we consider the

planar wing for the basic properties. Aerofoil section thickness remains constant at 7%.

### 3.1 Planar Wing

**Fig.9** shows longitudinal total forces ($C_L$ , $C_D$ , $C_A$) and pitching moment ($C_m$) variations. These are accompanied by spanwise loadings of $C_{LL}$, $C_{DL}$ and $C_{AL}$, over an Angle of Attack (AoA) range 0° to 5° in 1° steps. Spanwise loadings factored by the local to mean chord ratio ($c/c_{av}$) are also shown ($C_{LL}$. $c/c_{av}$, $C_{DL}.c/c_{av}$ and $C_{AL}.c/c_{av}$). The lift-curve slope is about 0.0560/°. This enables a choice of AoA and $C_L$ for design. The $C_A$ and $C_D$ curves are functions of $C_L^2$. $C_m$ is shown referred to three reference points, neutral point at Mach 0.8, neutral point at Mach 0.2 and 5% $c_{av}$ stable about neutral point at Mach 0.2. At Mach 0.8, $C_m$ about the neutral point is independent of $C_L$. The spanwise loadings enable an assessment of the local tip loadings that are important to understand on highly tapered wings with planform "cranks". The local loadings of $C_{LL}$ and $C_{AL}$ are "high" from y/s = 0.3 to the tip. The inner wing between y/s = 0 and 0.3 produces low lift intensity and hence more drag.

Similar distributions were obtained for the planar wing at Mach 0.2. The lift-curve slope is about 0.0472/°.

### 3.2 Designed Wing, Varying Static Margin

The design $C_L$ is chosen as 0.2 (AoA about 3.6°). **Fig.10** relates static margins and neutral point and centre of pressure location xcp at Mach 0.2 and 0.8. $C_m$ constraints are according to static margin = 0% $c_{av}$ (neutral stability), and ±5% $c_{av}$ (unstable and stable) referred to the Mach 0.2 Neutral Point.

The designed wing geometry for neutral stability is compared with the planar case in **Fig.11**. These are accompanied by spanwise distributions of $C_{LL}$, $C_{DL}$ and $C_{AL}$ with and without $c/c_{av}$ factor for AoA 0°(1°)5°. Further detail on the other static margin conditions is in Ref.16. The 0% $c_{av}$ stable case has 12.89° twist between wing root and wing tip, about 10.0° between root and y/s=0.8. The twist distribution has an implication on wing setting angles and fuselage incidence. The designed centre-line camber is favourable for incorporating a S-duct propulsion with top mounted intakes.

## 4. LAYOUT – U2

As before, the emphasis is on an appreciation of camber and twist required for varying stability at a design point of Mach 0.8 cruise, $C_L$ = 0.2. Aerofoil section thickness is set at 7%. First we consider the planar wing.

### 4.1 Planar Wing

**Fig.12** shows longitudinal total forces and pitching moment variations together with the spanwise loadings (AoA 0°(1°)5°). The lift-curve slope is about 0.0601/°. This enables a choice of AoA and $C_L$ for design. The $C_A$ and $C_D$ curves are functions of $C_L^2$. $C_m$ is shown referred to three reference points, neutral point at Mach 0.8, neutral point at Mach 0.2 and 5% $c_{av}$ stable about neutral point at Mach 0.2. At Mach 0.8, $C_m$ about the neutral point is independent of $C_L$. The local loadings of $C_{LL}$ and $C_{AL}$ increase steadily from root to tip as expected for this delta planform. This suggests a very tolerant wing at high AoA, less prone to tip-stall or wing-drop. The $C_{LL}c/c_{av}$ distribution is smooth and near-elliptic (low induced drag).

Similar distributions were obtained for the planar wing at Mach 0.2. The lift-curve slope is about 0.0513/°.

Upper surface Mach and $C_P$ contours together with $C_P$ distributions from Euler calculations, Mach 0.8, AoA = 2.5°, 3.0°, 3.5° and 4° are shown in **Fig.13**. Local Mach numbers in the range 0.8<M<0.9 dominate the upper surface with inboard and tip regions effectively unswept. More detail is in Ref.16.

### 4.2 Designed Wing, Varying Static Margin

The design $C_L$ is chosen as 0.2 (AoA about 3.3°). We look at designs with $C_m$ constraint according to static margin = 0% $c_{av}$ (neutral stability), and ±5% $c_{av}$ (unstable and stable) referred to the Mach 0.2 Neutral Point. The variation in centre of pressure location (xcp) for the three design cases is shown in **Fig.14**. Mach 0.2 and 0.8 neutral point locations are defined.

The designed wing geometry for neutral stability is compared with the planar case in **Fig.15**. This is accompanied by spanwise loadings (AoA 0°(1°)5°). The 0% $c_{av}$ stable case has 12.44° twist between wing root and wing tip. As mentioned in Ref.16, the magnitude of twist decreases as the design becomes less stable, 13.79° (stable), 12.44° (neutrally stable) and 11.08° (unstable).

The implication of twist distribution on wing setting angles is noted. The designed centre-line camber is favourable for incorporating a S-duct propulsion with top mounted intakes.

Upper surface Mach and $C_P$ contours together with $C_P$ distributions from Euler calculations on the designed geometry, Mach 0.8, AoA = 2.5°, 3°, 3.5° and 4° are shown in **Fig.16**. Local Mach numbers in the range 0.8<M<0.96 dominate the upper surface. The design camber and twist distributions have ensured that the contours are effectively swept across the semi-span. The tip region (y/s>0.85) is effectively unswept.

## 5. LAYOUT – U3

Again, the emphasis is on an appreciation of camber and twist required for varying stability at a design point of Mach 0.8 cruise, $C_L$ = 0.2. Aerofoil section thickness remains constant at 7%. First we consider the planar wing.

### 5.1 Planar Wing

**Fig.17** shows longitudinal total forces and pitching moment variations together with the spanwise loadings (AoA 0°(1°)5°). The lift-curve slope is about 0.0750/°. This enables a choice of AoA and $C_L$ for design. The $C_A$ and $C_D$ curves are functions of $C_L^2$.$C_m$ is shown referred to three reference points, neutral point at Mach 0.8, neutral point at Mach 0.2 and 5% $c_{av}$ stable about neutral point at Mach 0.2. At Mach 0.8, $C_m$ about the neutral point is independent of $C_L$. The local loadings of $C_{LL}$ and $C_{AL}$ are relatively "high" from y/s = 0.3 to the tip. The effects of coincident LE and TE cranks are evident and more pronounced than for U1. The latter has slightly offset LE/TE cranks and a highly swept fuselage chine. On U3, the inner wing between y/s = 0 and 0.4 produces low lift intensity and hence produces more drag.

Similar distributions were obtained for the planar wing at Mach 0.2. The lift-curve slope is about 0.0594/°.

Upper surface pressure and Mach contours and $C_P$ – x distributions from Euler calculations, Mach 0.8, AoA = 2°, 2.5° & 3° are shown in **Fig.18**. High sonic flows are predicted near the LE, even at low AoA. The unswept mid-chord regions are very evident. At AoA = 3°, the tip region exhibits typical shock flow distributions.

### 5.2 Designed Wing, Varying Static Margin

The design $C_L$ is chosen as 0.2 (AoA about 2.7°). We look at wing designs with $C_m$ constraint according to static margin = 0% $c_{av}$ (neutral stability), and ±5% $c_{av}$ (unstable and stable) referred to the Mach 0.2 Neutral Point. The variation in centre of pressure location (xcp) for the three design cases is shown in **Fig.19**. Mach 0.2 and 0.8 neutral point locations are defined.

The designed wing geometry for neutral stability is compared with the planar case in **Fig.20**. This is accompanied by spanwise loadings (AoA 0°(1°)5°).

The 0% $c_{av}$ stable case has 9.14° twist between wing root and wing tip. The magnitude of twist decreases as the design becomes less stable: 10.02° (stable), 9.14° (neutrally stable) and 8.25° (unstable). More details are in Ref.16.

The implication of twist distribution on wing setting angles is noted. The designed centre-line camber is favourable for incorporating a S-duct propulsion with top mounted intakes.

Upper surface pressure and Mach contours from Euler calculations on the designed geometry, Mach 0.8, AoA = 2°, 2.5° & 3° are shown in **Fig.21**. Local Mach numbers above 1.0 occupy very small areas just aft of the LE. Comparing with the planar case, the contours are effectively swept, across the semi-span, apart from the tip region (y/s>0.8).

## 6. LAYOUT – LJAST

The emphasis is on an appreciation of camber and twist required for the LJAST (Lambda Joined Wing with Aft Swept Tip) configuration at a design point of Mach 0.8 cruise, $C_L$ = 0.4. For this configuration, t/c remains constant at 7%. First we consider the planar wing.

### 6.1 Planar Wing

The configuration and aerofoil shape (uncambered) distribution is shown in **Fig.22**. Also shown are results from panel code calculations, spanwise distribution of $C_L$ c/cref for AoA 1.0 (0.5) 3.5, longitudinal total forces and pitching moment variations ($C_L$-□ and $C_m$-$C_L$) and chordwise pressure distributions at AoA = 1.5° and 3.0°. $C_m$ is slightly positive (requires some trimming) and $dC_m/dC_L$ is positive (unstable) over the $C_L$ range. The spanwise loadings show the component (Front, Rear and Tip wing) contributions, their summation and the equivalent elliptic distribution. From these initial results, a design $C_L$ of 0.4 (referred to front Wing Area) was selected with a target of near elliptic load distribution. At this $C_L$, the Cp distribution shows high LE suctions that may not be sustained and may lead to separated flow.

Upper surface pressure and Mach contours and $C_P$ – x distributions from Euler calculations, Mach 0.8, AoA = 0°, 1.5° and 3° are shown in **Fig.23**. There is good correlation between the panel and Euler codes results. The results broadly reflect the high local LE suctions. With further attention to Euler grids, it may be possible to improve the correlation further.

### 6.2 Designed Wing

The design $C_L$ is chosen as 0.4. The designed wing geometry is compared with the planar case in **Fig.24**. This is accompanied by spanwise loadings (AoA = -0.5°, 0.0° and 0.5°), total loads and chordwise pressure distributions. The front wing has positive twist at the root which fades to near zero at the join (y/s=0.7). The rear wing has positve twist from root to join. The outer wing has positive twist at the join fading to near zero at the tip. Varying degrees of positive camber are applied on all three wing components. Cm is now negative (requiring some additionl trimming) with $dC_m/dC_L$ positive (unstable). Again, stability and control issues can be addressed once fuselage and powerplant configurations have been established.

Euler results for the $C_L$=0.4 design case at Mach 0.8 and AoA –0.5, 0, +0.5 deg. (with respect to design angle) are shown in **Fig.25**. Apart from the need to improve on the aerofoil shaping (near the LE), these confirm broadly the design character inferred from the panel code.

## 7. LAYOUTS & COMPARISONS, LIFT, DRAG

### 7.1 Flying Wings, Lift & Drag

Linear theory lift-curve slope correlations with standard formulae based on half-chord sweep (Ref.5, Kucheman, Ref.36, McCormick and Ref.37, Raymer) are shown in **Fig.26** for Mach 0.8 and 0.2. The Mach 0.8 results, indicate that planforms U1 and U2 (AR=3.2) have effective sweeps of 35° and 30° respectively. U3 (AR=5.1) has effective sweep of 25°. The results correlate well with the theory. At low speed, M<0.3, compressibility and sweep effects are negligible.

The $C_L$□ - M variation, for the three planforms, is shown in **Fig.27**. The corresponding incidences required for cruise $C_L$ of 0.2, take-off $C_L$ of 0.6 and typical landing $C_L$ of 0.4 are shown in **Fig.28**. The benefits of high AR are evident. U1 requires near 13° rotation at take-off compared to U2, 11.6° and U3 requiring only10°. On landing at Mach 0.2, U1 might require 8° rotation, U3 less than 7°.

The variations of induced drag factor ($k = \pi AR\ C_{Di}/ C_L^{\ 2}$), for the three planforms at the same design condition ($C_L$=0.2, Mach 0.8, 5% $c_{av}$ stable, referred to the Mach 0.2 Neutral Point) are shown in **Fig.29**. Also shown are the effective 0% and 100% attained suction limits for each planform. At the design point, Mach 0.8, $C_L$ = 0.2, planform U2 achieves the lowest k value. This had been intimated by the near elliptic spanwise loadings resulting from the near delta planform. The approximate suction levels are 95%, 97% and 94% respectively. However, the significantly higher AR of U3

results in almost 30% lower induced drag compared with U1 and U2. The design $C_L$ is comparatively low and consequently the wave drag is very low. There is room for increased accuracy however, in the quest for increasing the range efficiency.

The variations of k, for the three design cases at Mach 0.2 are shown in **Fig.30**. Again, the 0% and 100% attained suction limits are shown. We consider two possible low-speed $C_L$ requirements, 0.4 and 0.6. At $C_L$ = 0.4 (landing) U2 achieves 61% suction level, U1 60% and U3 57%. At $C_L$ = 0.6 (take-off) U2 achieves 43% suction and both U1 and U3 achieve 40%. The higher AR of U3 results in significantly lower drag levels at low speed.

A total drag breakdown estimate for cruise (M=0.8, $C_L$=0.2) is shown in **Fig.31**. To the Induced drag ($C_{Di}$) for each planform an estimate of skin friction drag ($C_{DoSF}$) on the wing surfaces has been added. The variation in the remaining zero lift drag term ($C_{DoOTHER}$), attributable to intakes, excrescences, etc., is shown for various L/D values. $C_{Di}$ for U3 is significantly lower than for the other two planforms. This allows a greater "freedom" in terms of $C_{Do}$ for a given L/D.

### 7.2 Joined Wing Configuration, Lift & Drag

The lift curve slope variation with Mach number is shown in **Fig.32**. Results based on front wing area and total planform area are presented for both 7% and 15% t/c aerofoils. The corresponding AoA required for Cruise $C_L$=0.4, Take-Off $C_L$=1.3 and Landing $C_L$=1.2 for the 7% thick cases are shown in **Fig.33**. To achieve the required lift at take-off, the design requires an additional rotation of almost $10^o$. Just over $8^o$ rotation is required on landing.

The variations of Lift induced drag factor ($k = \pi AR\, C_{Di}/C_L^2$) for design $C_L$ = 0.4 and also 0.2 are shown in **Fig.34**. The effective 0% suction level is indicated. Possible separated flow regions are shown.

Keeping $C_{Do}$ within desirable limits and also its initial evaluation are notoriously difficult. Estimates of total drag breakdown for the $C_L$=0.2 and 0.4 designs, with varying $C_{Do}$ levels (0.016 to 0.024), are shown in **Fig.35**. Lift induced drag ($C_{Di}$) has been estimated for each case at the design condition. To this is added a skin friction term ($C_{DoSF}$) and a further zero lift drag term ($C_{DoOTHER}$) attributable to intakes, etc. The corresponding L/D achieved are indicated. **Fig.36** shows the variation of L/D for each design case with a similar range of $C_{Do}$ values. For UAV and UCAV configurations, L/D in the region of 15 may be typical.

## 8. PERFORMANCE ESTIMATIONS

### 8.1 Breguet Range & Performance

The Breguet Range Equation (e.g. Ref.38) for Equivalent Still Air Range (ESAR) is:

$$ESAR = L/D \times V/sfc \times \ln(W1/W2)$$

Where W1 = Initial Mass, W2 = Final Mass = W1 – WF, WF relates to Fuel used.

L/D is the Lift to Drag ratio and V is the aircraft speed (kt).

sfc is the specific fuel consumption of the installed engine (lb/hr/lb).

Endurance (hours) can be found from ESAR / V.

Useful expressions for relating Payload (WP) and Operating Empty weight (OEW) are:

TOW = OEW + WP + WF, WF/TOW = 1 - W2/W1, TOW = WF/(1 - (OEW + WP)/TOW)

The total flight distance or ESAR assumes that all the fuel on board is consumed. Safety margins allow for changes in fuel consumption rates (engine malfunction, weather, altitude adjustments, etc.) or enforced diversions (loss of destination airfield, weather, tactical decisions, etc.). Jenkinson's correlation for relating the ESAR to the Design Range (R) is:

ESAR = 568 + 1.06 x R (nm).

For shorter range, military and experimental aircraft, it may be more reasonable to use a modified form e.g.:

ESAR = 284 + 1.06 x R (nm).

The maximum TOW is usually a structural limitation of the aircraft. For passenger aircraft and military strike aircraft it is a compromise between fuel required for a given payload and range combination. WP depends on the combat role (a part or all may be released). OEW is

fixed and WF is limited by the capacity of the fuel tanks or the maximum TOW.

### 8.1 Flying Wings

The X-45A is a relatively small, development aircraft with TOW between 12,000 lb and 15,000 lb. The quoted OEW/TOW is 0.53 with payload varying from 1500 lb up to 3000 lb. An endurance capability of between 90 minutes and 3 hours is claimed. This implies that its cruise endurance may be reduced by about 50 minutes taking into account the climb and descent phases. A Breguet range formulation will need to be fairly detailed as L/D during climb and descent are likely to be different and lower from those at cruise. We have made an attempt to show the variation of TOW with Endurance and Range for the U1 configuration in **Fig.37** with simplifications, e.g. M = 0.75 at 36,000ft, OEW/TOW=0.55, WP=3000 lb, sfc = 1.00 and 1.05, for various values of L/D between 7 and 12. It is interesting to see that for the quoted TOW of 12000 and 15000 lb, the endurance of the aircraft varies between 1.4 and 3.4 hours, depending on L/D and sfc. Such a figure gives a feel for various quantities but we need to include more details about the flight envelope, L/D and sfc variations as functions of speed.

TOW for the X-45C and X-47B aircraft are of the order of 36500lb and 42000lb respectively with ranges of 2600nm and 3000nm. For the U2 and U3 configurations, variations of TOW with design Range for L/D between 11 and 15 are shown in **Fig.38**. These assume M = 0.8 at 36,000ft, sfc 0.85 and OEW/TOW values of 0.50 and 0.55. WP is 4500 lb. With OEW/TOW = 0.55, the U2 configuration requires L/D of 14.0 for an endurance range of 3000 nm. Under these conditions, configuration U3 requires an L/D of just over 13 for the same range. Reducing OEW/TOW to 0.50 (more advanced materials) U2 requires L/D of only 11.5 and U3 10.5 for a 3000 nm range. From these estimates we are able to establish allowable $C_{Do}$ values.

### 8.2 Joined Wing Configuration, Lift & Drag

We have attempted to illustrate the variation in TOW with endurance (hr) and Range (nm) for a range of L/D values in **Fig.39** assuming OEW/TOW = 0.50, V = 460 kt (Mach 0.8) and WP = 5000 lb for sfc = 0.9 and 1.0. In the current work no fuel allowances for contingencies have been made, endurance is based on the full fuel load. **Fig.40** shows similar trends but for OEW/TOW = 0.55. In the latter case, for an endurance of just under 10 hr, L/D would need to be over 20 (very low $C_{Do}$) and sfc = 0.9 and the resulting UCAV would have TOW = 50,000 lb. Using more advanced materials in the construction might reduce OEW/TOW to 0.5. A UCAV with TOW = 40,000 lb, less efficient engines (sfc = 1.0) would also have an endurance of just under 10 hr, **Fig.39**. This type of TOW – Range diagram illustrates the "trade-offs" that can be used to achieve a certain Range or endurance. The importance of achieving high L/D is evident.

Although much further work remains to be done, it would appear that this configuration can offer better overall performance than the flying wing layouts considered so far.

Further project work can now be done with a greater confidence level. The process described can be extended for design with additional constraints; stability margins, structural bending and torsion can be introduced.

## 9. INFERENCES, CONCLUDING REMARKS & FURTHER WORK

There is a revival of interest in flying wings for military (and civil) use. The military context arises from "stealthy" HALE and UCAV requirements. There has also been renewed interest in the joined wing concept and its application to high AR, long endurance surveillance UAVs. The joined wing concept may also be developed into the UCAV role.

Questions on aerodynamics, control and structural efficiency arise. For flying wings, without a trim surface, the constraints on the wing pitching moment (trim stability margins) dictate the design camber and twist. This aspect needs to be understood in detail when comparing different types of planforms. Control power requirements can be high because of the effectively short moment arms. Compared with

conventional wing / tail arrangements, flying wings have a special set of very different constraints. The joined-wing configuration offers high AR and at the same time considerable scope for flying controls location. However, the relatively narrow wings may involve strength and structural rigidity issues.

This paper has been concerned with the study of four configurations (three flying wings and a joined wing) for UCAV applications. It was inspired by the need to understand a variety of wings (in public domain) that are, at first sight, aimed at similar missions. The main emphasis has been on developing and understanding cruise design camber and twist with neutrally stable constraint. Spanwise lift and drag loadings have also been presented. Camber design has been via attained thrust methods and a modal approach. The verification of the design approach is via Euler results that confirm reasonably benign behaviour of the designs.

The joined wing layout could provide an attractive option for UCAV's. With more detailed studies it may be possible to develop it for multi-roles incorporating some of the HALE (Sensorcraft) functions.

### Possible Future Work

Several avenues for future work have arisen e.g.

- using closely "tailored" design modes, e.g. omitting powerplant and weapons bay areas.
- integration of power-plant (intake flow, engine sizing, exhaust flow).
- Consideration of more varied layouts including forward swept wings (FSW), for parametric studies.
- Combining optimised camber and twist with transonic Euler studies.
- pitch trim, including low-speed leading and trailing edge flap (LEF & TEF) effects.
- control power requirements which can be high because of "effectively" small moment arms on flying wings.
- off-design aspects, e.g. sideslip and / or manoeuvring flight (take-off, landing, weapon release, combat, etc.).
- detailed performance / envelope sttudies

The approach followed in this paper is readily applicable to "Morphing" Wing Configurations (**Fig.41**) that are being currently proposed by DARPA in USA.

## ACKNOWLEDGEMENTS

The work mentioned here is part of in-house R & D activities. The authors have pleasure in acknowledging helpful technical discussions with Mr. R.H. Doe, Prof. J.E. Cooper (UK), Dr. C.P. Tilmann & Dr. M. Blair (US-AFRL). Opportunities for collaboration are invited.

Lastly it should be mentioned that any opinions expressed are those of the authors. Co-operation and sponsorship is warmly invited.

## REFERENCES

1. LIEBECK, R.H., PAGE, M.A. & RAWDON. B.K., "Blended-Wing-Body Subsonic Commercial Transport", AIAA-98-0438, Jan. 1998.
2. ROMAN, D., ALLEN, J.B. & LIEBECK, R.H., "Aerodynamic Design Challenges of the Blended-Wing-Body Subsonic Transport", AIAA-2000-4335, Jan. 2000.
3. WOLKOVITCH, J., "The Joined Wing: An Overview", J. of Aircraft, Vol 23, pp. 161-178, March 1986.
4. WOLKOVITCH, J., "A Second Look at the Joined Wing", Proc. of NVVL Symposium "Unconventional Aircraft Concepts", Delft Uni. Press, 1987.
5. KUCHEMANN, D. "The Aerodynamic Design of Aircraft", Pergamon.
6. JUPP, J., "Wing aerodynamics and the Science of Compromise", RAeS Lanchester Lecture, 2001.
7. JONES, R.T., "Wing Theory", Princeton.
8. NANGIA, R.K. & PALMER, M.E., "Flying Wings (Blended Wing Bodies) With Aft & Forward Sweep, Relating Design Camber & Twist to Longitudinal Control", AIAA-2002-4616, August 2002.
9. NANGIA, R.K., PALMER, M.E. & TILMANN, C.P., "On Design of Unconventional High Aspect Ratio Joined-Wing Type Aircraft Configurations", ICAS 2002-25R2, Toronto, Canada.
10. NANGIA, R.K., PALMER, M.E. & TILMANN, C.P., "Towards Design and Optimisation of Unconventional High Aspect Ratio Joined-Wing Type Aircraft Configurations", CEAS Conference, June 2002, Cambridge UK.
11. NANGIA, R.K., PALMER, M.E. & TILMANN, C.P., "Unconventional High Aspect Ratio Joined-Wing Aircraft with Aft- & Forward- Swept Wing-Tips", AIAA-2003-0605, Jan. 2003, Reno, USA.
12. NANGIA, R.K., PALMER, M.E. & TILMANN, C.P., "Unconventional High Aspect Ratio Joined-Wing Aircraft Incorporating Laminar Flow", AIAA-2003-3927, June 2003, Orlando, USA.
13. NANGIA, R.K., "Towards Designing Novel High-Altitude Joined-Wing Sensor-Craft (HALE-UAV)", AIAA Paper 2003-2695, AIAA/ICAS Wright Brothers. Centennial, Dayton, OH, USA, July 2003.
14. NANGIA, R.K., PALMER, M.E. & TILMANN, C.P., "Towards Design of a Novel High-Altitude Joined-Wing Sensor-Craft (HALE-UAV)", 19th Bristol

Unmanned Air Vehicle Systems Conference, 29-31 March 2004.

15. NANGIA, R.K., PALMER, M.E. & TILMANN, C.P., "Planform Effects on Unconventional High Aspect-Ratio Joined-Wing Aircraft Incorporating Laminar Flow". AIAA-Paper, 2005-0243, 43rd AIAA Aerospace Sciences Meeting, Reno, January 2005.
16. NANGIA, R.K. & PALMER, M.E., "A Comparative Study of Several UCAV Type Wing Planforms – Aero Performance & Stability Considerations", Paper AIAA-2005-5078, 23rd Applied Aerodynamics Meeting, Toronto, Canada, June 2005.
17. NANGIA, R.K. & PALMER, M.E., "Joined Wing Configuration for High Speeds – A First Stage Aerodynamic Study", Paper Proposed for AIAA Aerospace Sciences Meeting, Reno Jan. 2006.
18. CARLSON, H.W., SHROUT, S.L., & DARDEN, C.M., "Wing Design with Attainable Leading-Edge Thrust Considerations"., AIAA Jo. of Aircraft, Vol.22, No.3, pp 244-8, Marc 1985.
19. PLOTKIN, A. & KATZ, J. "Low-Speed Wing Theory", Wiley, (Formalized Theory for Panel Codes).
20. GUPTA, K.K. & MEEK, J.L., "Finite Element Multidisciplinary Analysis", AIAA, 2000.
21. NANGIA, R.K., "Development of an Inverse Design Technique using 3-D Membrane Analogy", Future Paper.
22. NANGIA, R.K., "Low Speed Performance Optimisation of Advanced Supersonic Civil Transport with Different LE & TE Devices", EAC'94, Toulouse, France, Oct.94.
23. NANGIA, R.K., "The Design of Manoeuvrable" Wings using Panel Methods, Attained Thrust & Euler Codes", ICAS-92.
24. NANGIA, R.K. & GREENWELL, D.I., "Wing Design of an Oblique-Wing Combat Aircraft", ICAS-2000-1.6.1.
25. NANGIA, R.K., PALMER, M.E. & GREENWELL. D.I., "Design of Conventional & Unconventional Wings for UAV's", RTO-AVT Symp, "UV for Aerial & Naval Military Operations", Turkey, Oct. 2000.
26. NANGIA, R.K., PALMER, M.E. & DOE, R.H., "A study of Supersonic Aircraft with Thin Wings of Low Sweep", AIAA 2002-0709, Jan.2002.
27. NANGIA, R.K., PALMER, M.E. & TILMANN, C.P. (AFRL), "Design of High Aspect Ratio "Lambda-Wings" Incorporating Laminar Flow ", AIAA-2004-1245, 42nd AIAA Aerospace Sciences Meeting, Reno, January 2004.
28. NANGIA, R.K., PALMER, M.E. & TILMANN, C.P. (AFRL), "Design of High Aspect Ratio Double-crank "Lambda-Wings" Incorporating Laminar Flow ", AIAA Paper, 2004-2141, 4th AIAA Fluid Dynamics June 2004, Portland, Oregon, USA.
29. NANGIA, R.K. & GALPIN, S.A., "Towards Design of High-Lift Krueger Flap Systems with Mach & Re Effects for Conventional & Laminar Flow Wings", CEAS European Forum, Bath, UK, 1995.
30. NANGIA, R. K. & GALPIN, S.A., "Prediction of LE & TE Devices Aerodynamics in High-Lift Configurations with Mach & Reynolds No. Effects", ICAS-1996-2.7.6.
31. NANGIA, R.K. & MILLER, A.S. "Vortex Flow Dilemmas & Control on Wing Planforms for High Speeds", RTO AVT Symp, Loen, Norway, May 2001.
32. NANGIA, R.K., PALMER, M.E. "Unconventional Joined-Wing Concept for Supersonic Aircraft", Paper 24, RTO-AVT-99 Conference, Brussels, April 2003.
33. NANGIA, R.K., PALMER, M.E. & IWANSKI, K.P. (AFRL), "Towards Design of Long-range Supersonic Military Aircraft", AIAA Paper, 2004-5071, Providence Rhode Island, USA, 2004.
34. NANGIA, R.K., PALMER, M.E. & DOE, R.H., "Towards Design of Mach 1.6+ Cruise Aircraft", AIAA Paper, 2004-5070, Providence, RI, USA, 2004
35. NANGIA, R.K., PALMER, M.E. & IWANSKI, K.P. (AFRL), "Towards Design of Long-range Supersonic "Large" Military Aircraft", RAeS Paper 16, Sept. 2004, London, UK.
36. McCORMICK, B.W. "Aerodynamics Aeronautics and Flight Mechanics", Wiley.
37. RAYMER, D.P., "Aircraft Design – A Conceptual Approach", AIAA, 2003.
38. JENKINSON et al, "Civil Jet Aircraft Design", Arnold, 1999.

## NOMENCLATURE

| | |
|---|---|
| AR | Aspect Ratio |
| b | = 2 s, Wing span |
| c | Local Wing Chord |
| $c_{av}$ | = $c_{ref}$ = S/b, Mean Geometric Chord |
| $C_A$ | = Axial force/(q S), Axial Force Coefficient |
| $C_{AL}$ | Local Axial Force Coefficient |
| $C_D$ | = Drag Force /(q S), Drag Coefficient |
| $C_{DL}$ | Local Drag Coefficient |
| CG | Centre of Gravity |
| $C_L$ | = Lift Force/(q S), Lift Coefficient |
| $C_{LL}$ | Local Lift Coefficient |
| $C_m$ | = m/(q S $c_{av}$), Pitching Moment Coefficient |
| $C_{mL}$ | Local Pitching Moment Coefficient |
| $C_P$ | Coefficient of Pressure |
| LE, TE | Leading Edge, Trailing Edge |
| LEF, TEF | Leading Edge Flap, Trailing Edge Flap |
| L/D | Lift to Drag ratio |
| m | Pitching moment |
| M | Mach Number |
| q | = 0.5 ρ $V^2$, Dynamic Pressure |
| Re | Reynolds Number, based on $c_{av}$ |
| s, S | semi-span, Wing Area |
| V | Free-stream Velocity |
| $x_{AC}$ | Chordwise position of Aerodynamic Centre |
| α | AoA, Angle of Attack |
| ß | $\sqrt{(M^2-1)}$ |
| Λ | LE Sweep Angle |
| η | = y/s, Non-dimensional spanwise Distance |
| ρ | Air Density |

FIG.1 PROPOSED AND EXISTING FLYING WING CONFIGURATIONS

Military
Flying Wings

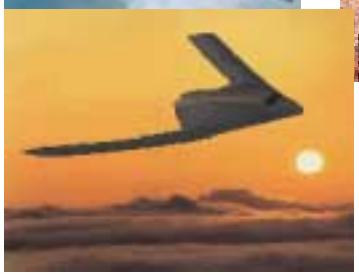

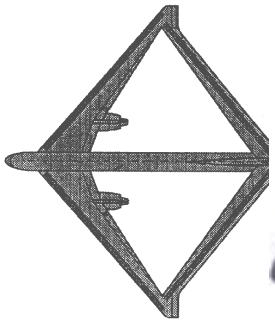

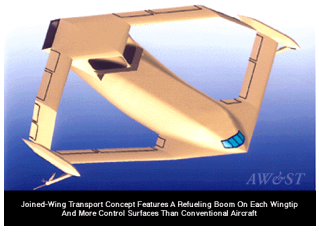


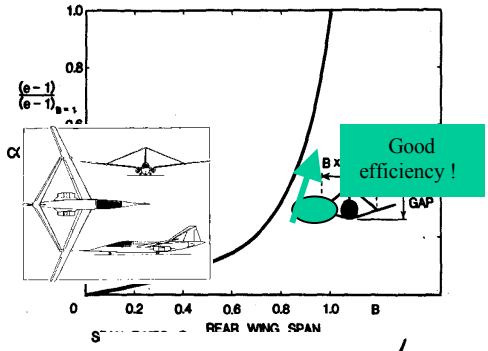


Good efficiency !

FIG. 2 SEVERAL RECENT JOINED-WING APPLICATIONS

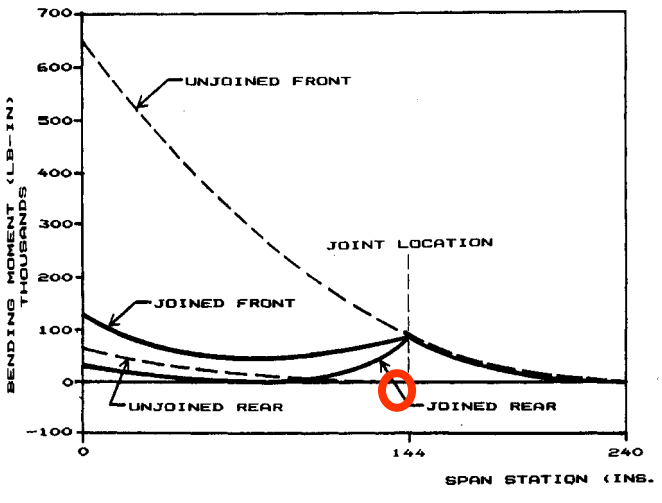


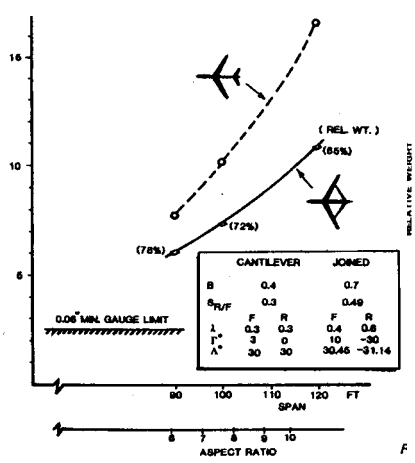


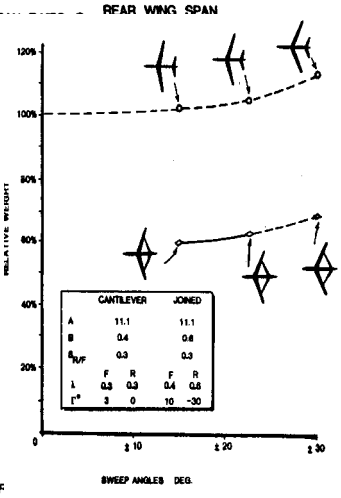


Fig. 3 JOINED WING STRUCTURAL ADVANTAGES

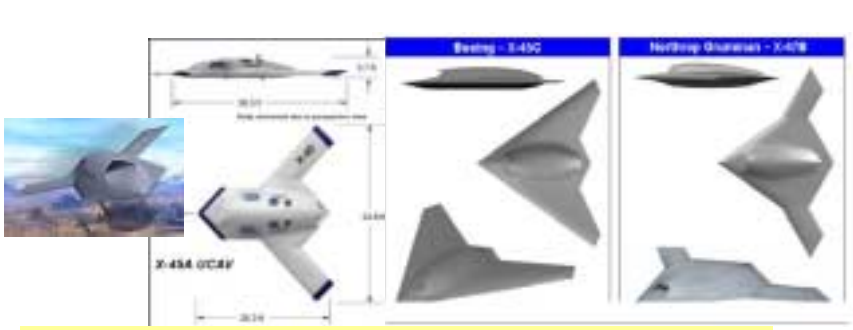


FIG.4 TYPICAL CURRENT FLYING WING UCAV PROJECTS

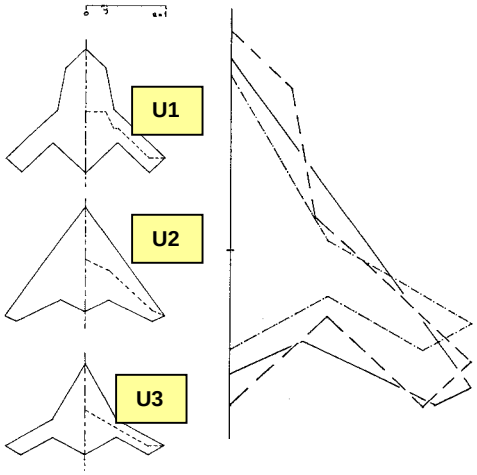


FIG.5 UCAV WING PLANFORMS COMPARED ON SIZE AND EQUAL-SPAN BASIS

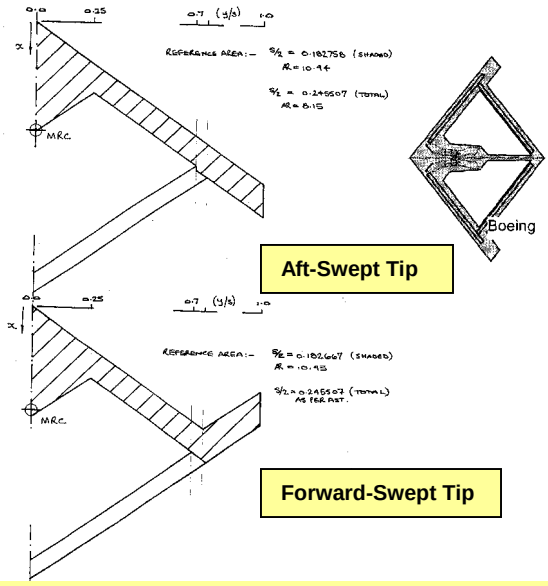


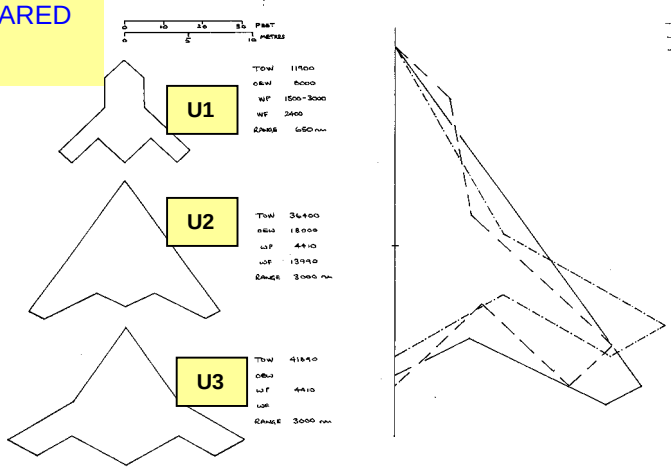


FIG. 7 JOINED WINGS - GEOMETRY PARAMETERS

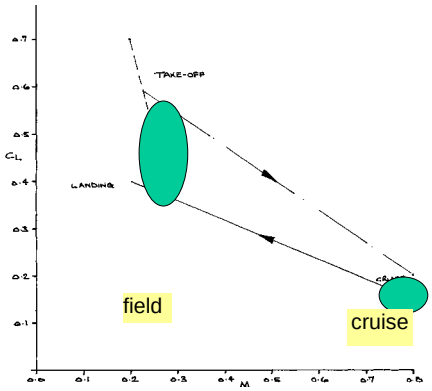


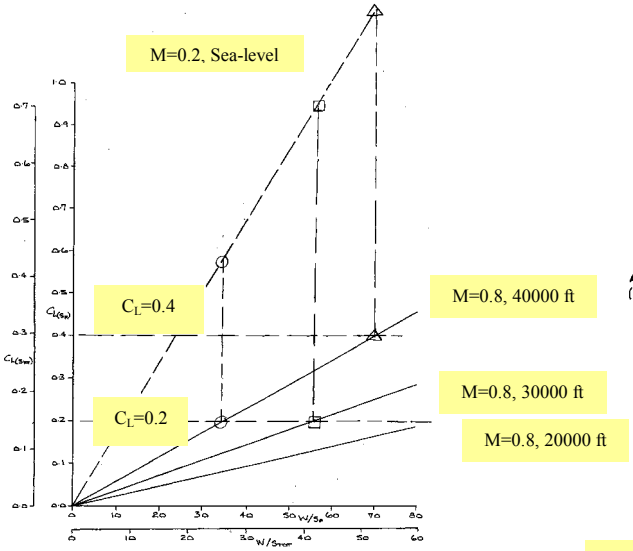


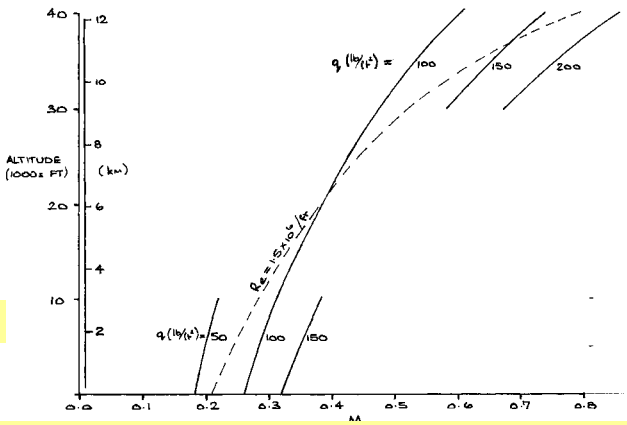


FIG. 8 WING LOADING, FLIGHT ALTITUDE & $C_L$ RELATIONSHIPS AT Mach 0.8

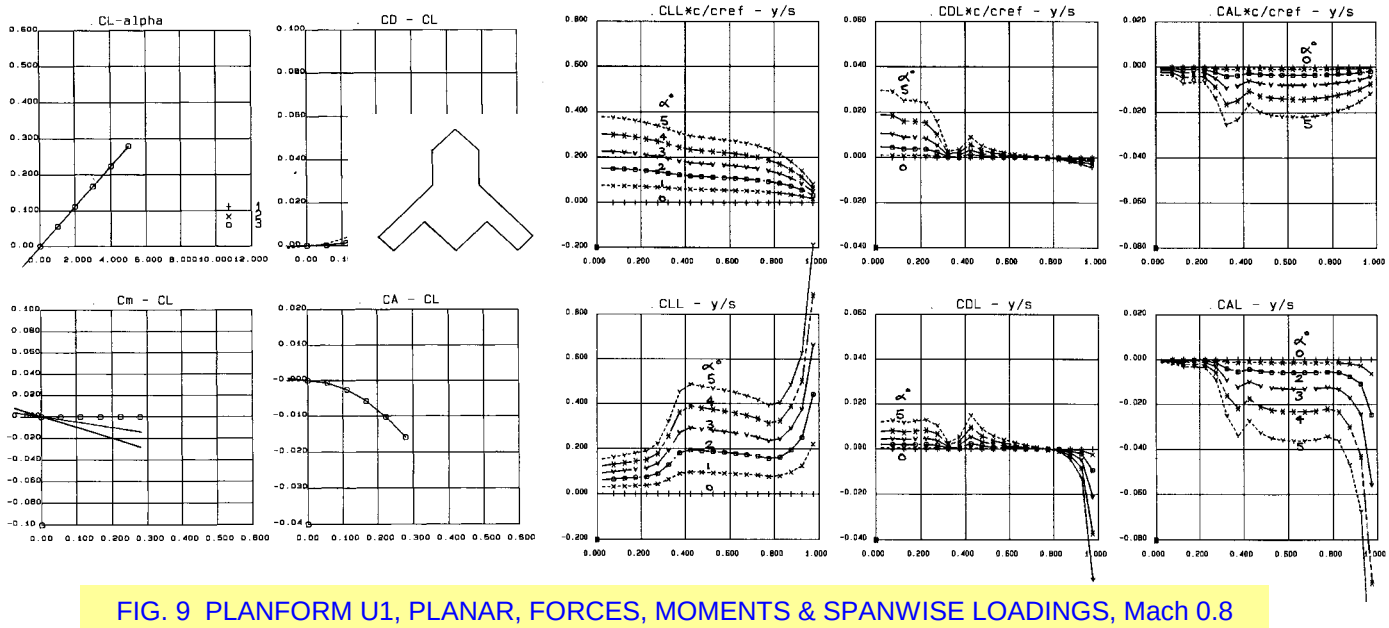


FIG. 9 PLANFORM U1, PLANAR, FORCES, MOMENTS & SPANWISE LOADINGS, Mach 0.8

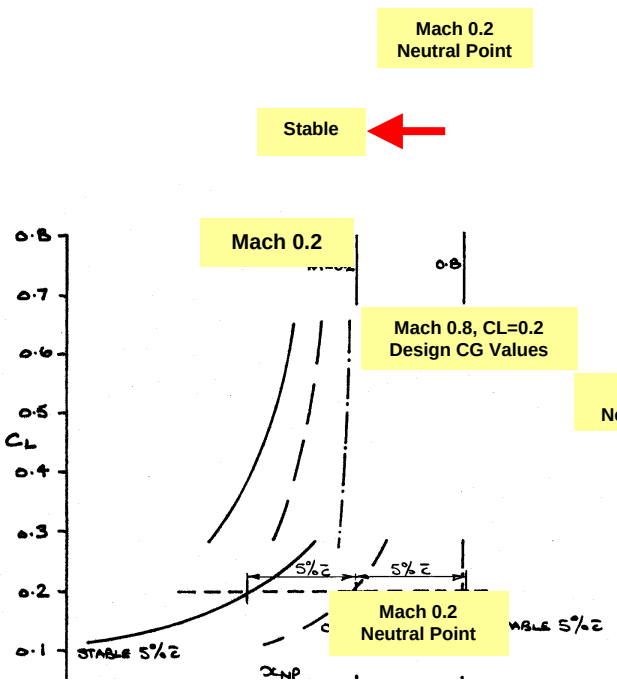


FIG. 10 U1 - RELATING STABILITY MARGINS, xcp Variation with CL, LOW-SPEED (Mach 0.2) and HIGH-SPEED (Mach 0.8), Linear Theory

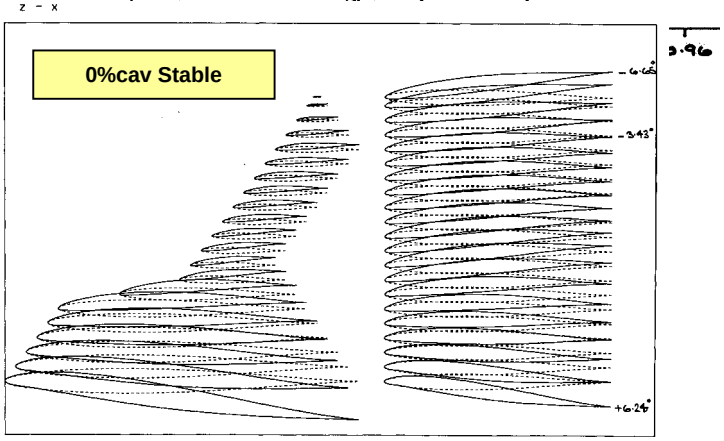


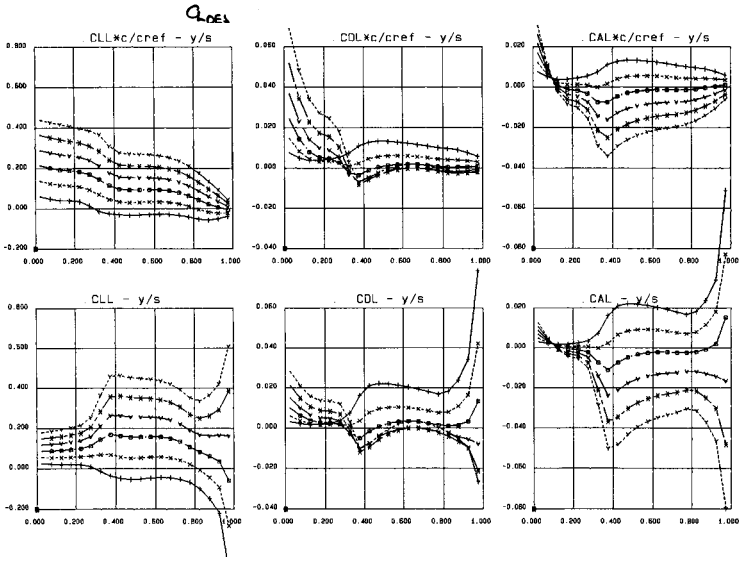


FIG. 11 PLANFORM U1, DESIGNED FOR $C_L$ = 0.2, $C_m$ = 0.0 at Mach 0.8, NEUTRAL STABILTY, Mach 0.8

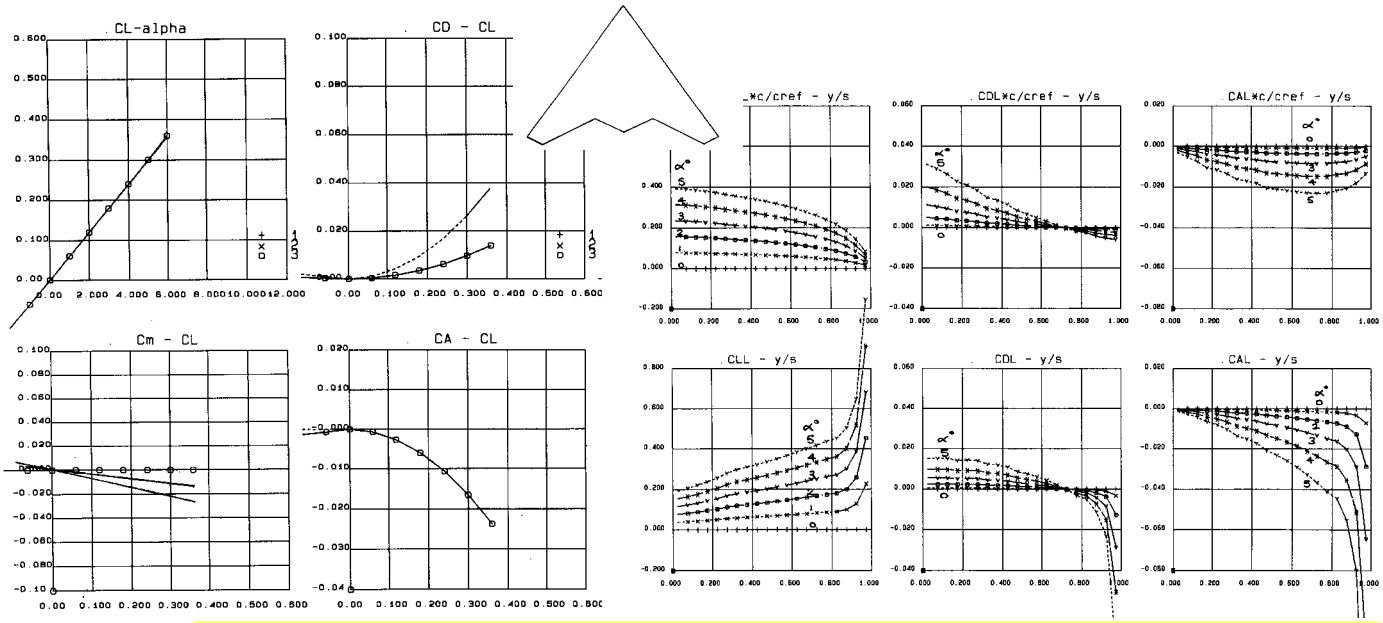


FIG. 12 PLANFORM U2, PLANAR, FORCES, MOMENTS & SPANWISE LOADINGS, Mach 0.8

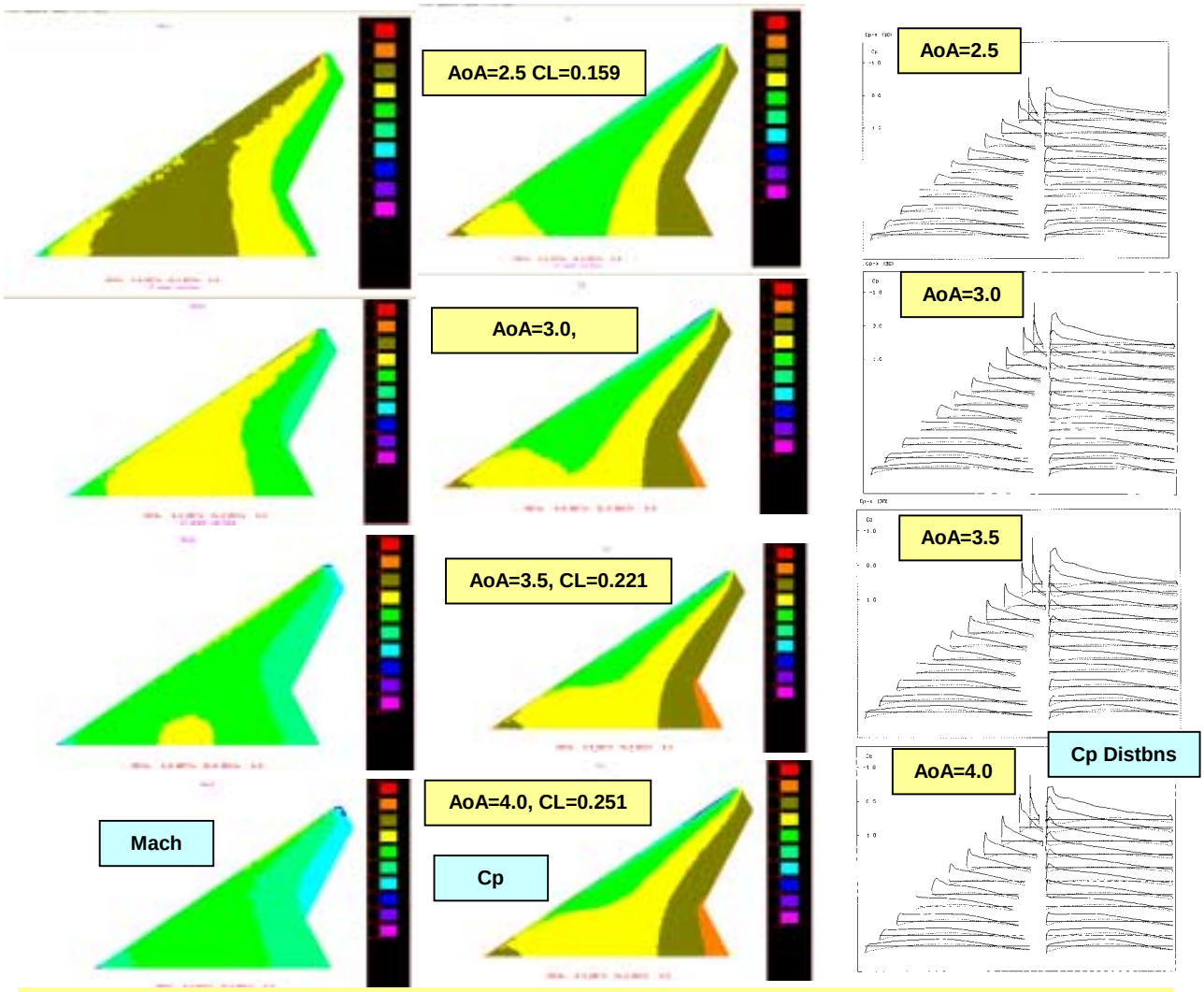


FIG. 13 PLANFORM U2, PLANAR, Mach 0.8, EULER, Mach & Cp Distbns, AoA 2.5, 3.0, 3.5 & 4.0

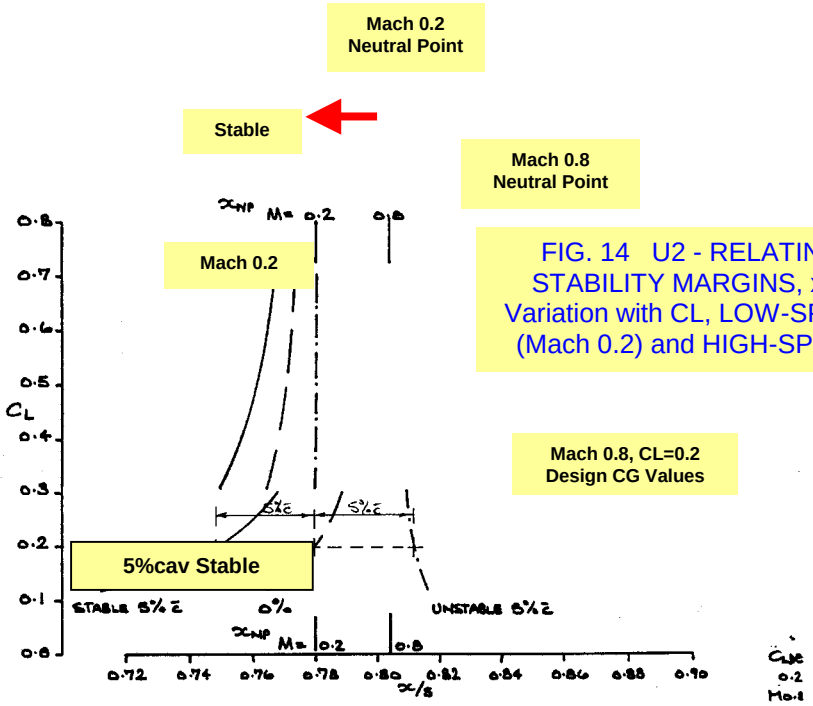


FIG. 14 U2 - RELATING STABILITY MARGINS, xcp Variation with CL, LOW-SPEED (Mach 0.2) and HIGH-SPEED

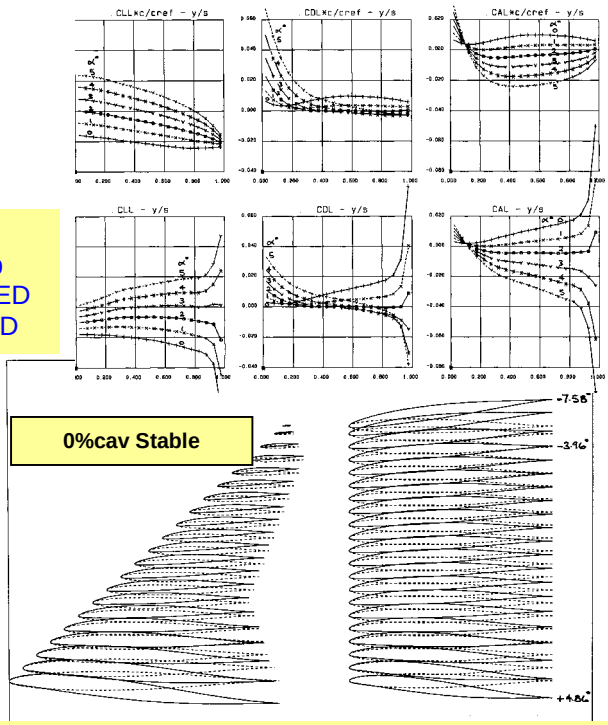


FIG. 15 PLANFORM U2, DESIGNED FOR $C_L$ = 0.2, $C_m$ = 0.0 at Mach 0.8, NEUTRAL STABILITY, Mach 0.8

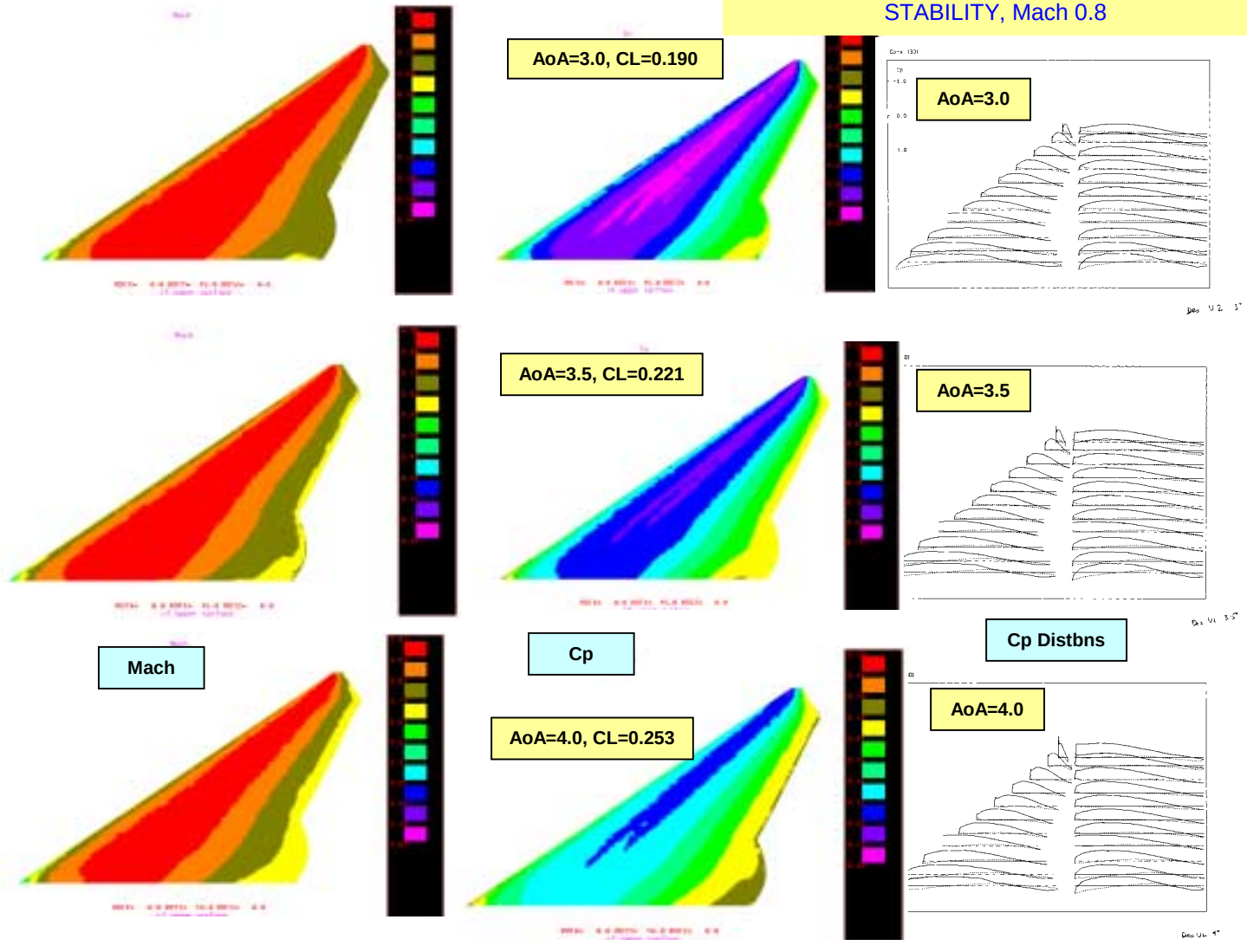


FIG. 16 PLANFORM U2, DESIGNED Mach 0.8, AoA 3.0°, 3.5° & 4.0°

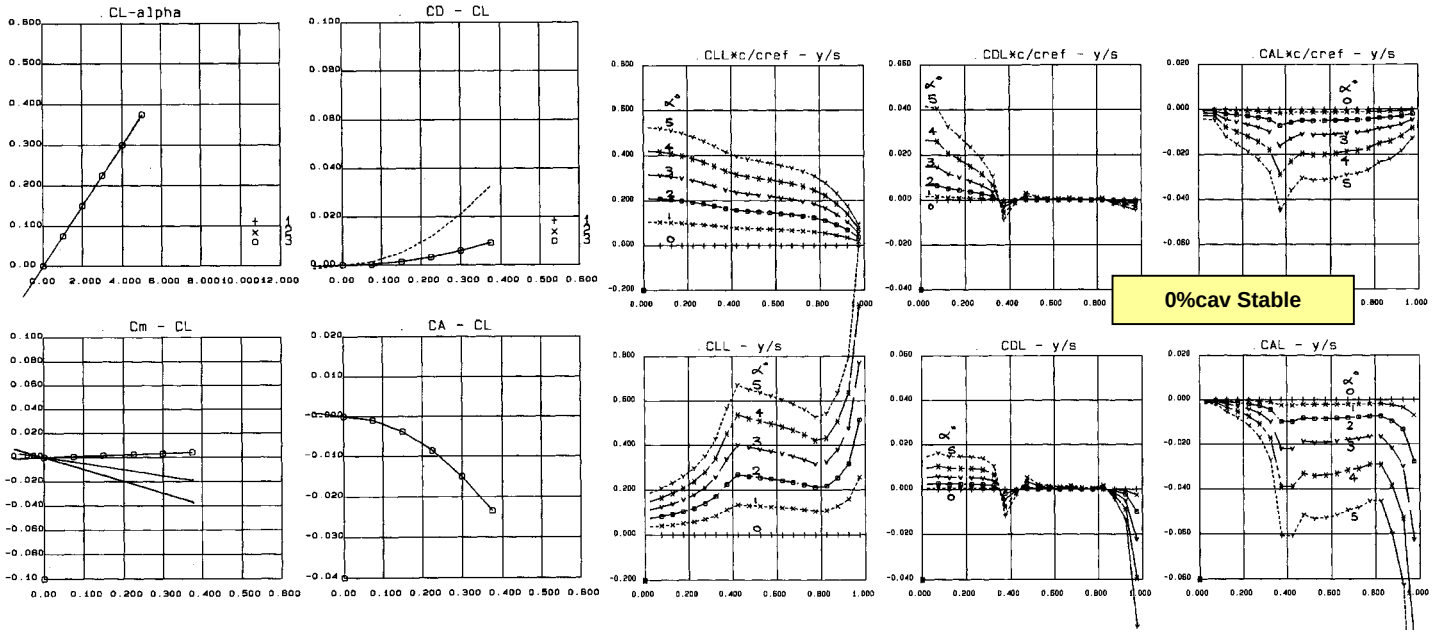


FIG. 17 PLANFORM U3, PLANAR, FORCES, MOMENTS & SPANWISE LOADINGS, Mach 0.8

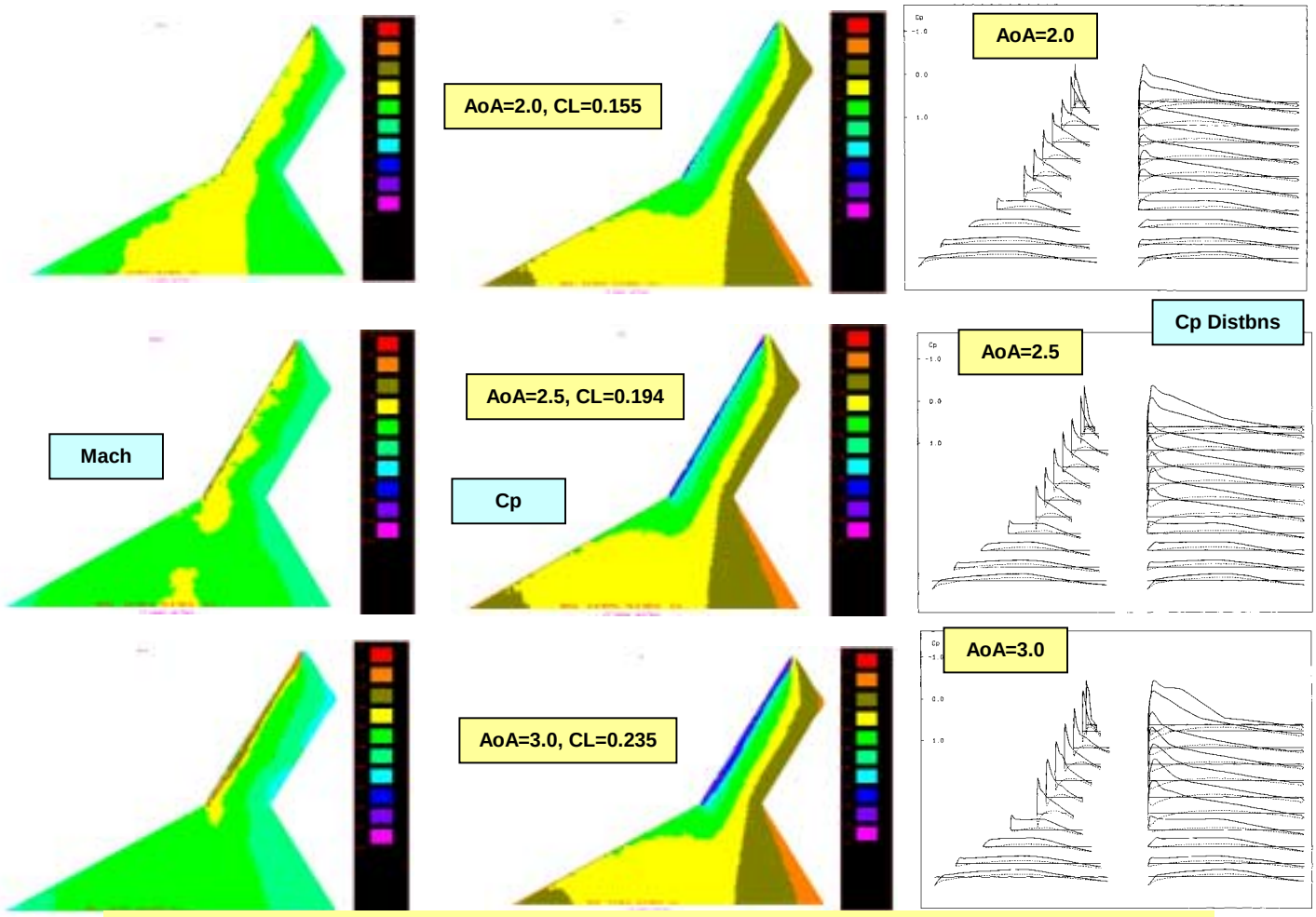


FIG. 16 PLANFORM U2, DESIGNED Mach 0.8, AoA 2.0°, 2.5° & 3.0°

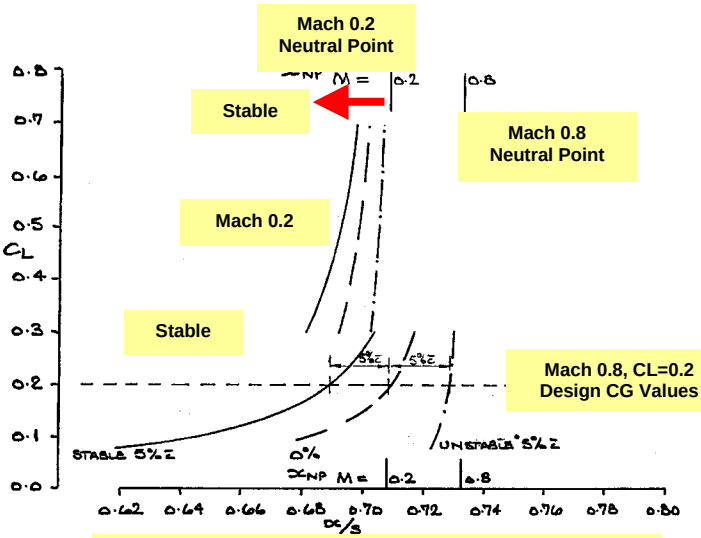


FIG. 19 U3 - RELATING STABILITY MARGINS, xcp Variation with CL, LOW-SPEED (Mach 0.2) and HIGH-SPEED (Mach 0.8), Linear Theory

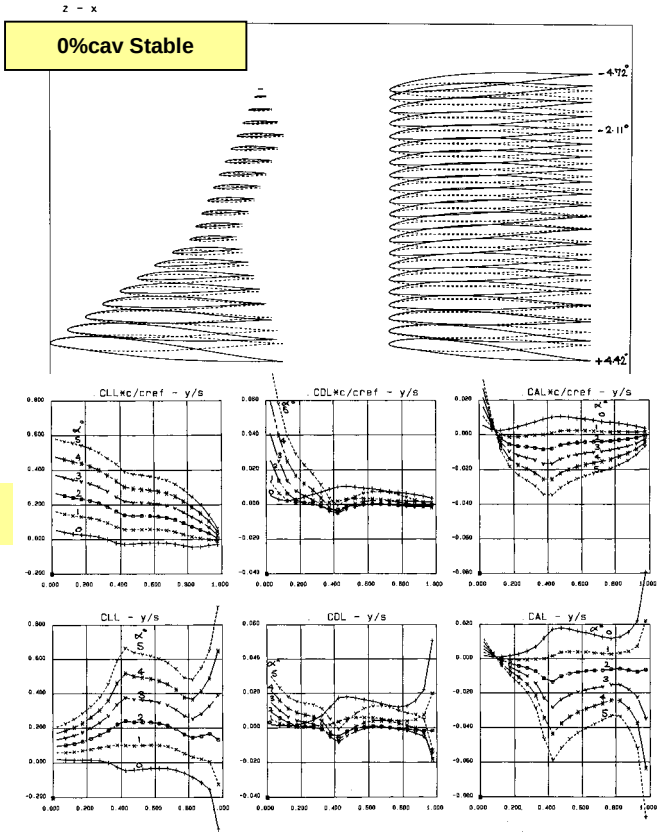


FIG. 20 PLANFORM U3, DESIGNED FOR $C_L$ = 0.2, $C_m$ = 0.0 at Mach 0.8, 0%smc STABLE (NEUTRAL

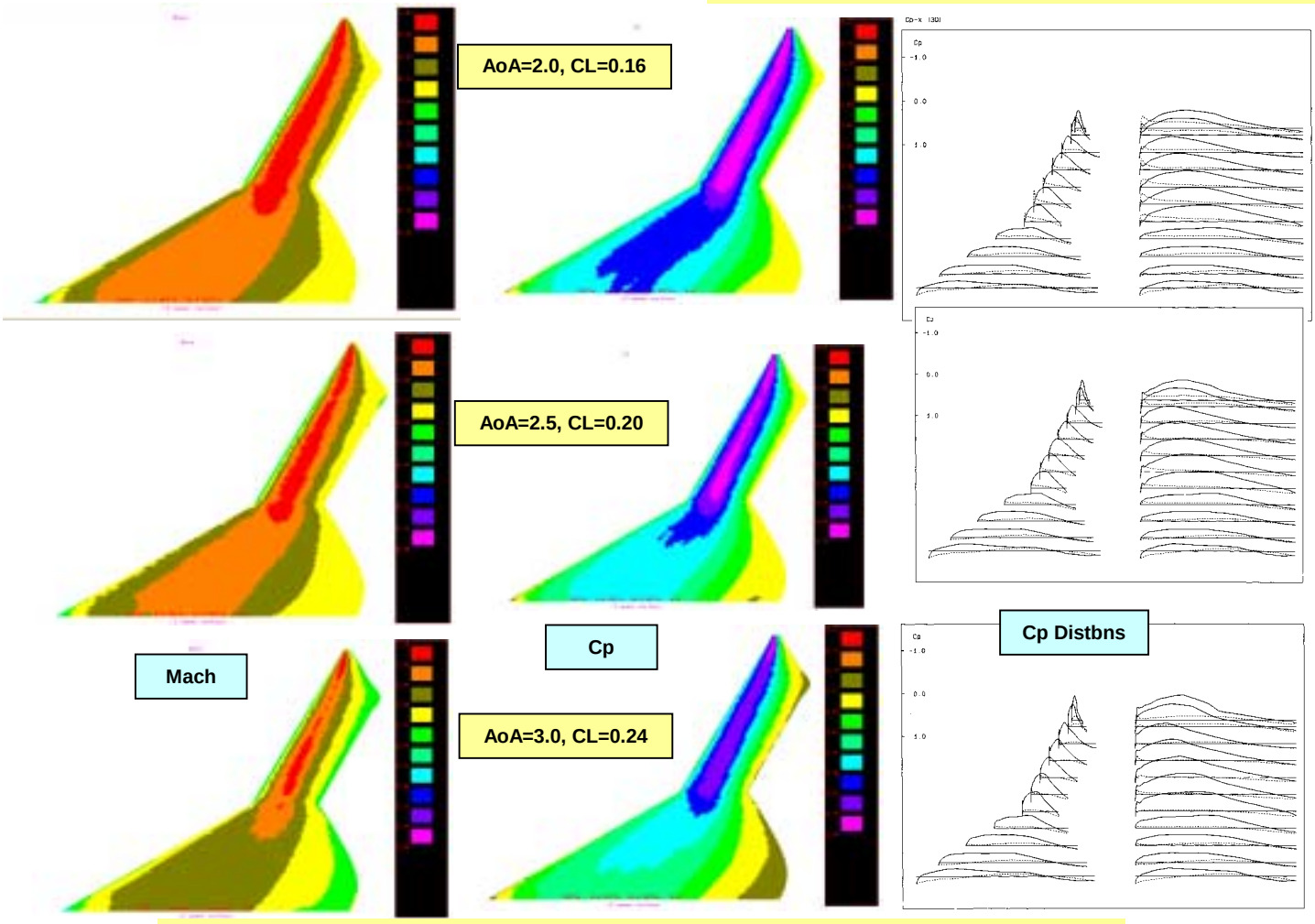


FIG. 21 PLANFORM U3, PLANAR, AoA 2.0°, 2.5° & 3.0°, Mach 0.8

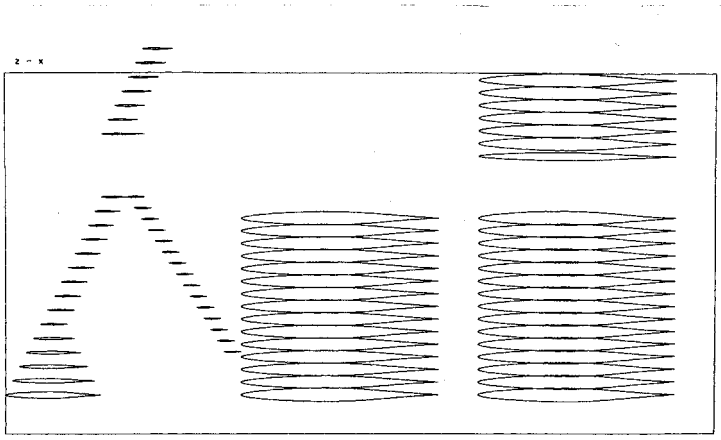

(a). UNCAMBERED AEROFOIL SHAPES

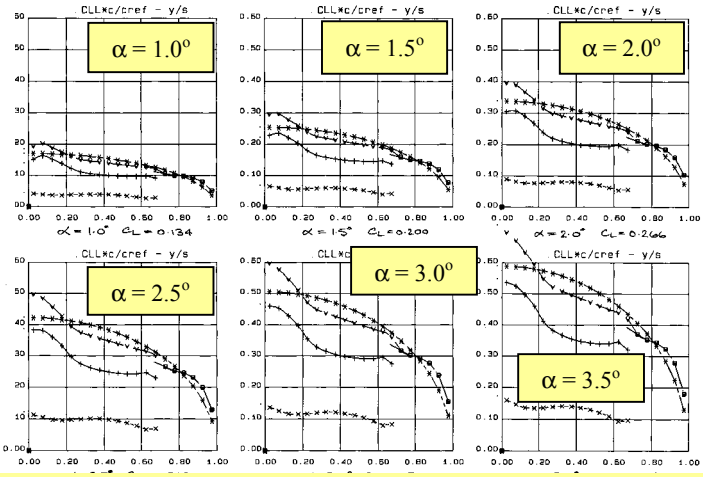


(b). SPANWISE LOADINGS THROUGH AoA RANGE, Mach 0.8
(Total compared with elliptic)

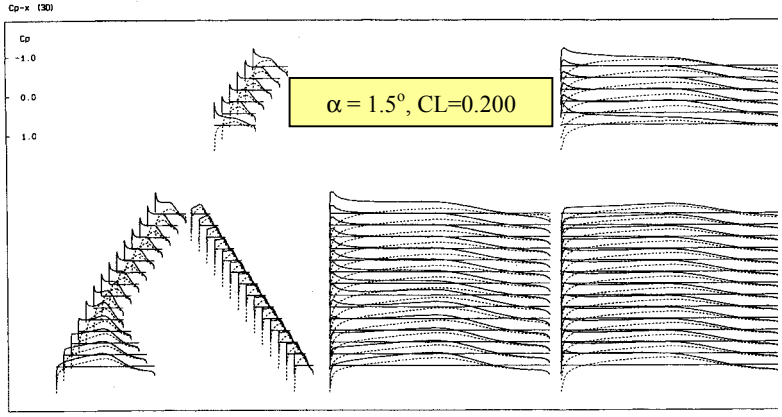


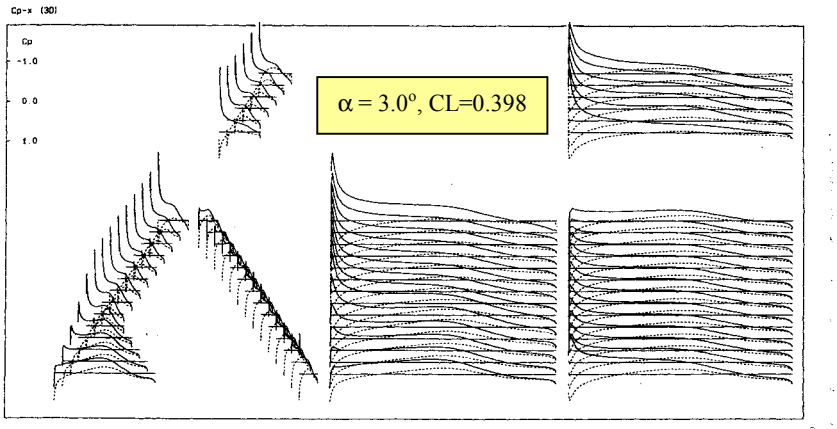


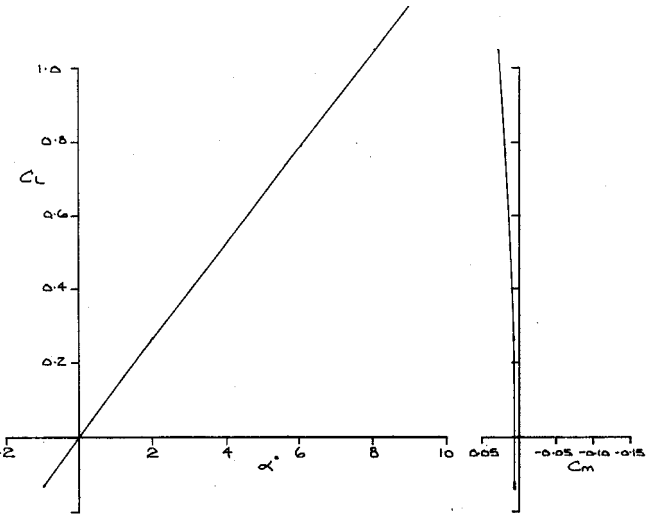


(c). CL & Cm Characteristics

FIG. 22 PLANFORM U3, DESIGNED , AoA 2.0°, 2.5° & 3°, Mach 0.8

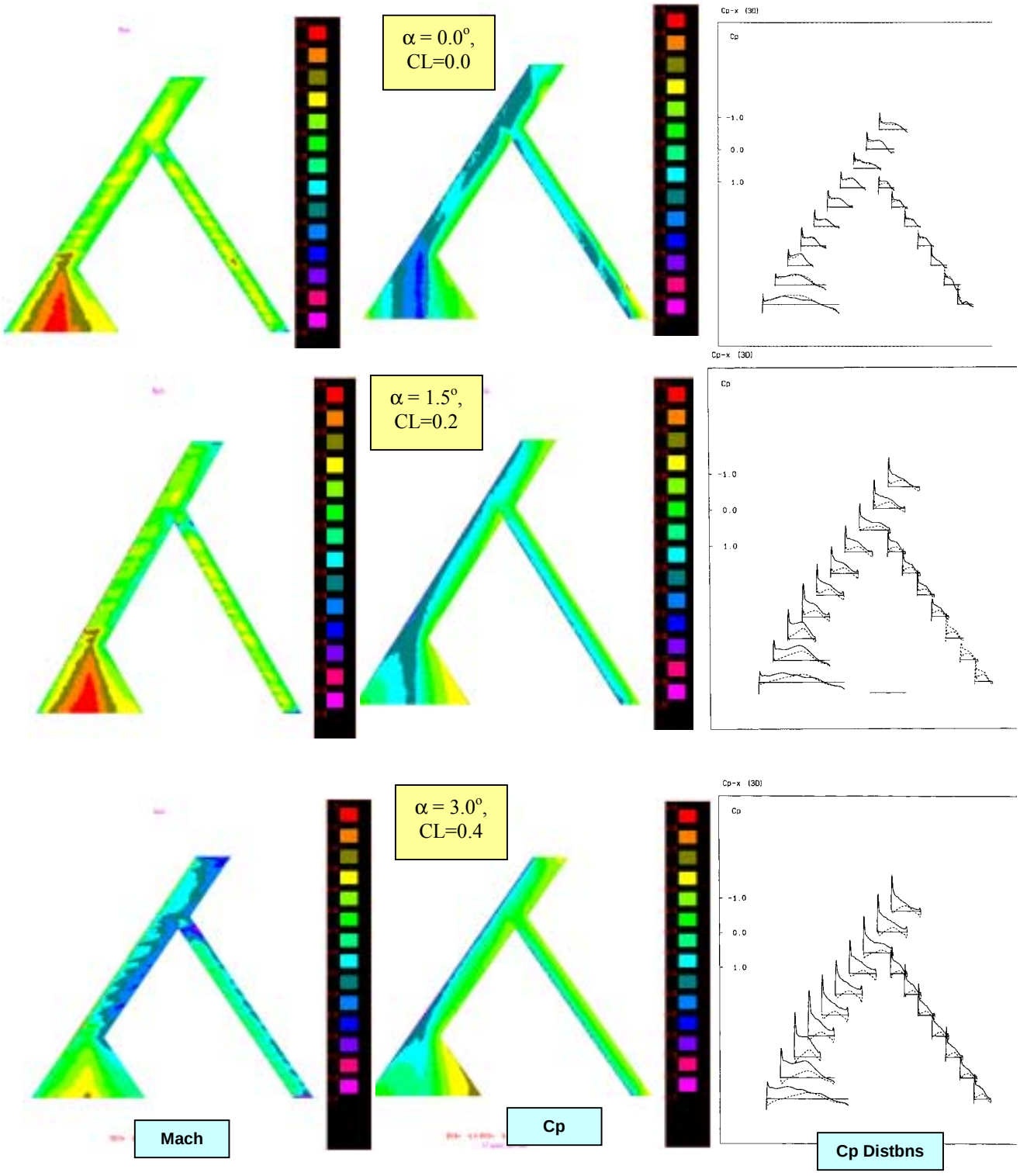


UNCAMBERED WINGS, Mach & Cp DISTRIBUTIONS THROUGH AoA (CL) RANGE, Mach 0.8, EULER

FIG. 23 CONFIG. LJAST

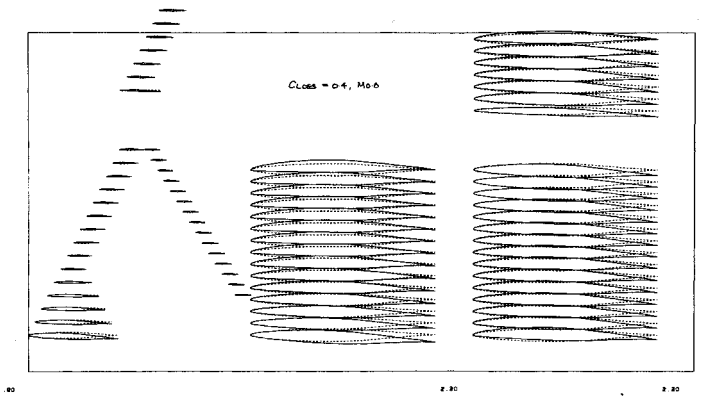


(a). UNCAMBERED & DESIGNED CAMBER (CL = 0.4) SHAPES

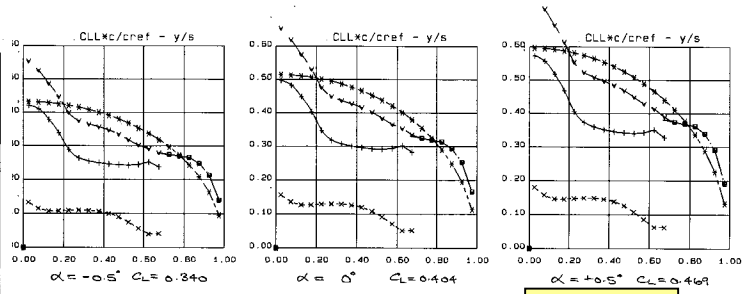


α = -0.5°

α = 0.0°

α = 0.5°

(b). DESIGN CAMBER (CL = 0.4), SPANWISE LOADINGS THROUGH AoA RANGE, Mach 0.8 (Total compared with elliptic)

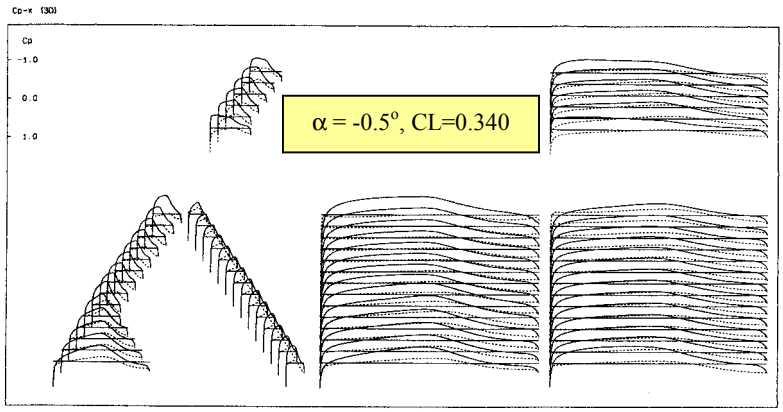


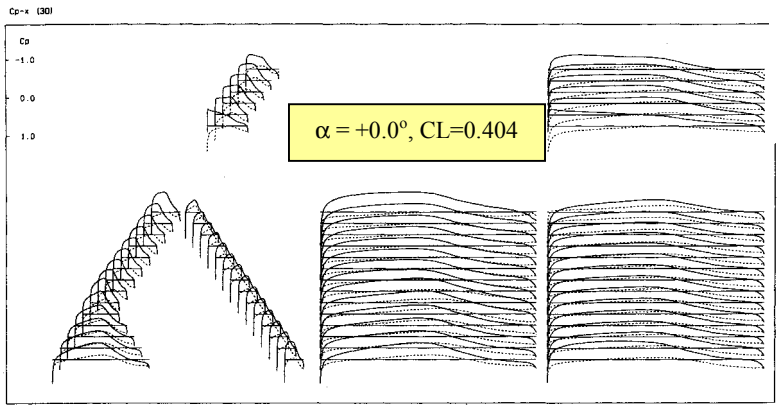


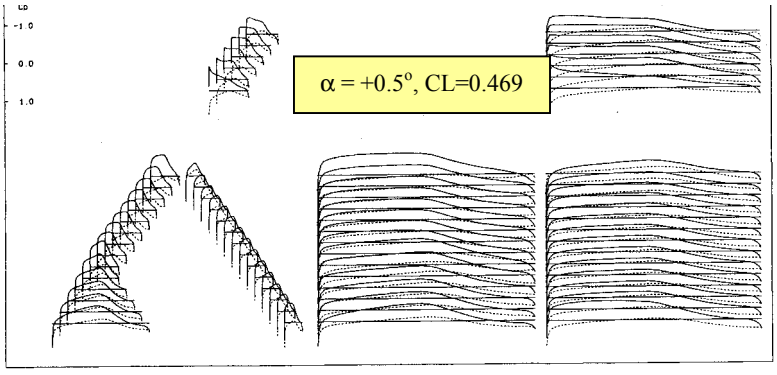


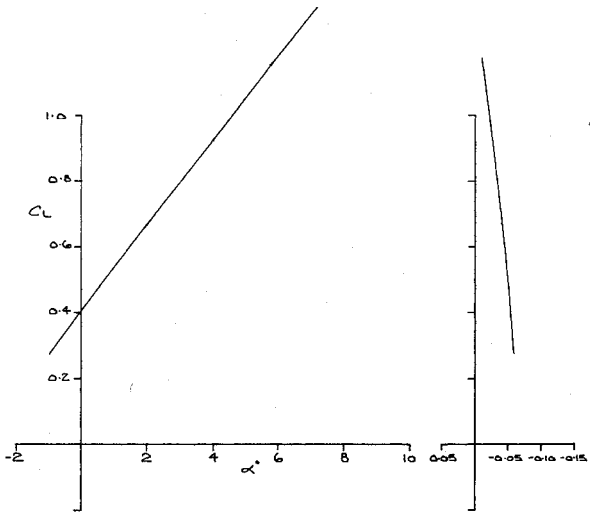


(c). CL & Cm Characteristics

(d) UNCAMBERED WINGS, Cp DISTRIBUTIONS THROUGH AoA (CL) RANGE, Mach 0.8

FIG. 24 CONFIG. LJAST

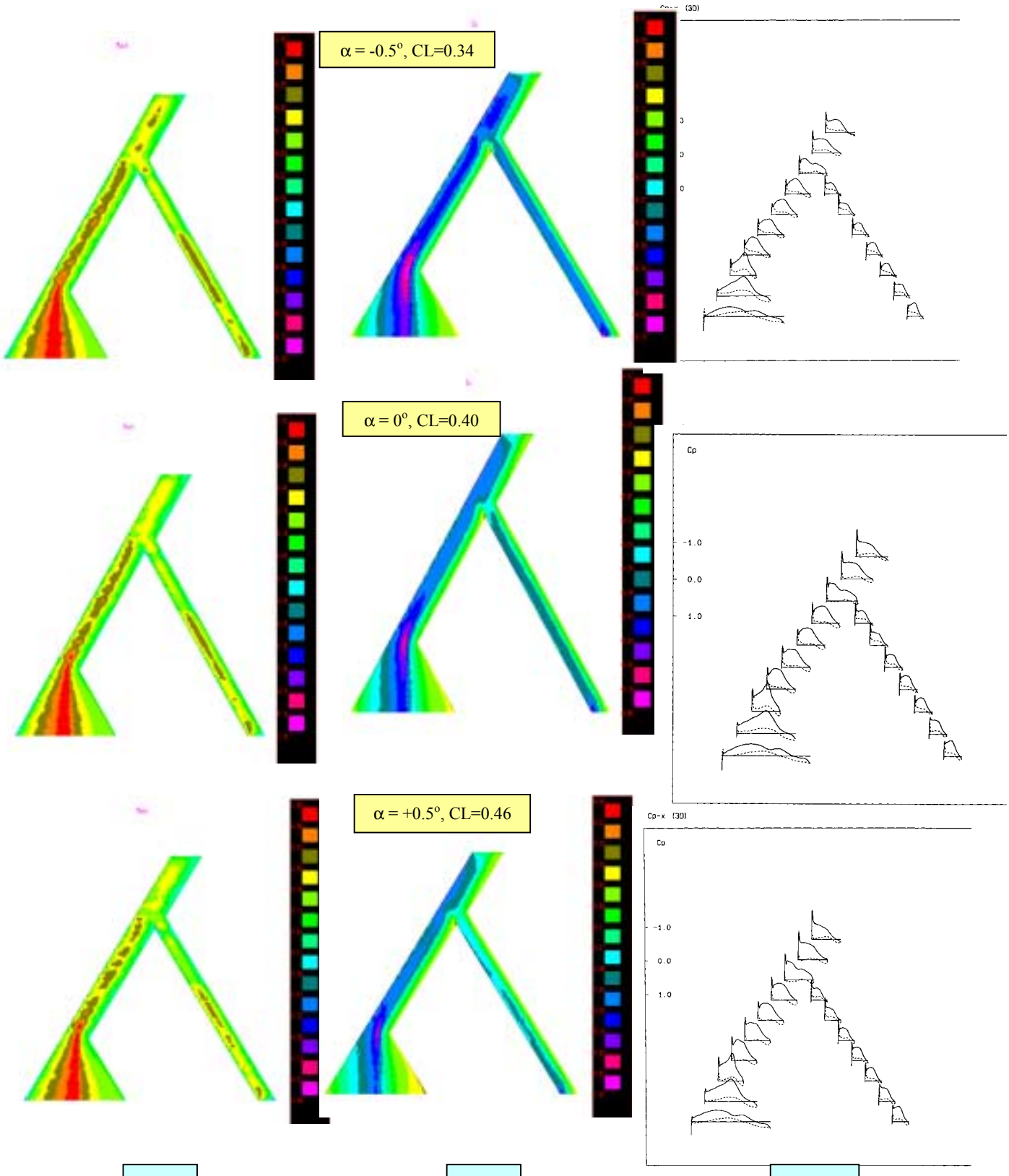


DESIGNED CAMBER, Mach & Cp DISTRIBUTIONS THROUGH AoA (CL) RANGE, Mach 0.8, EULER

FIG. 25 CONFIG. LJAST, CL = 0.4 Design

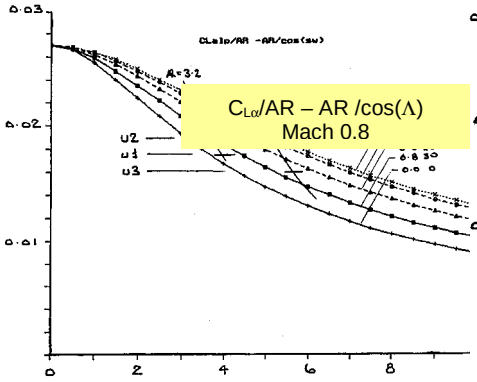


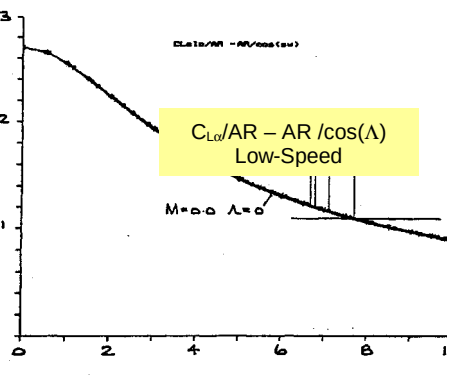


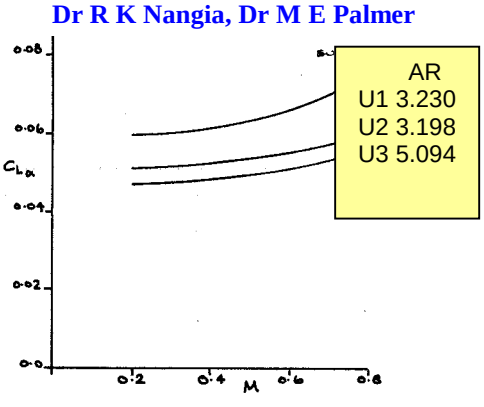


FIG. 26 THEORY, $C_{L\alpha}$ , AR & SWEEP RELATIONSHIPS COMPARED WITH RESULTS FOR LAYOUTS U1, U2 & U3, Mach 0.8 and Low speed

FIG. 27 VARIATION OF $C_{L\alpha}$ WITH M, PLANFORMS U1, U2 & U3

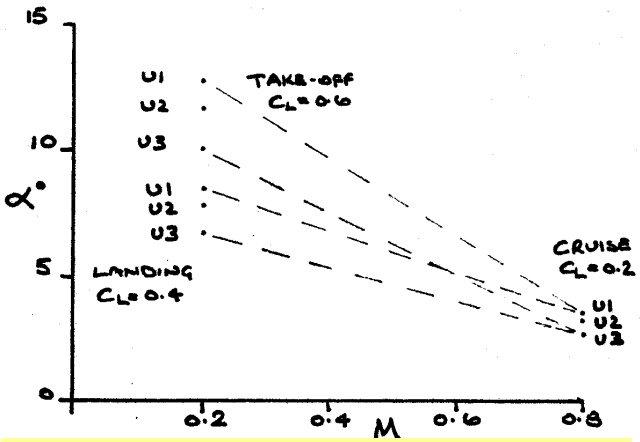


FIG. 28 INCIDENCE REQUIRED AT TAKE-OFF, CRUISE & LANDING, PLANFORMS U1, U2 & U3

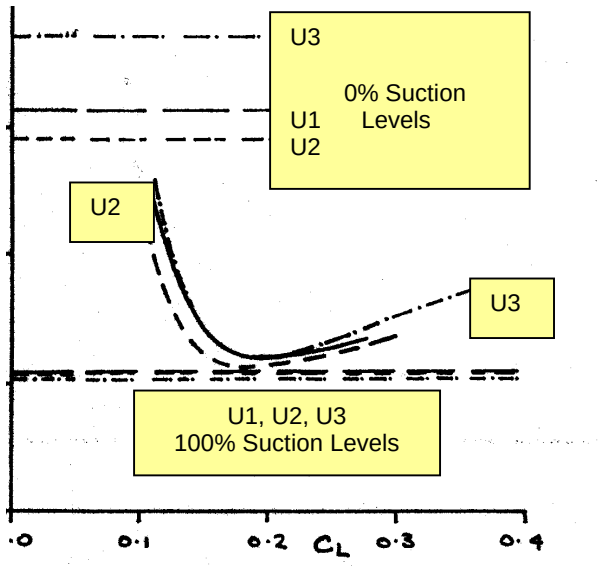


FIG. 29 VARIATION OF LIFT INDUCED DRAG FACTOR (k) WITH $C_L$, PLANFORMS U1, U2 & U3. Mach 0.8 DESIGN

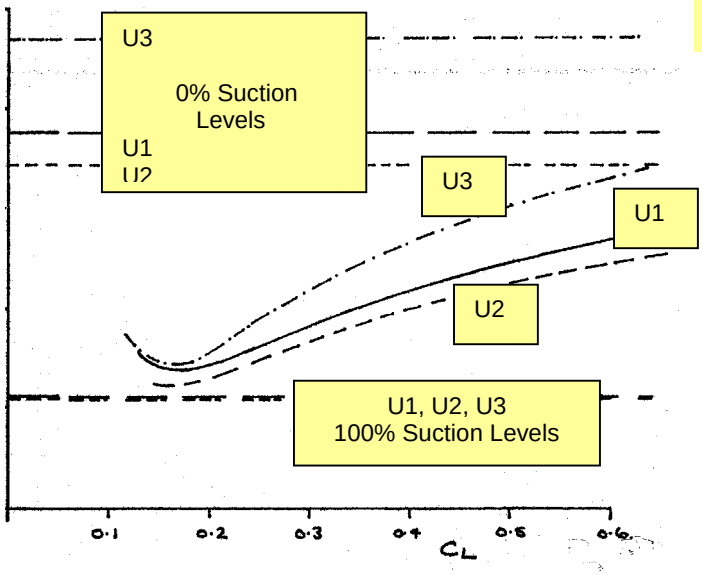


FIG. 30 VARIATION OF LIFT INDUCED DRAG FACTOR (k) WITH $C_L$, PLANFORMS U1, U2 & U3 (Mach 0.8 DESIGN), Mach 0.2

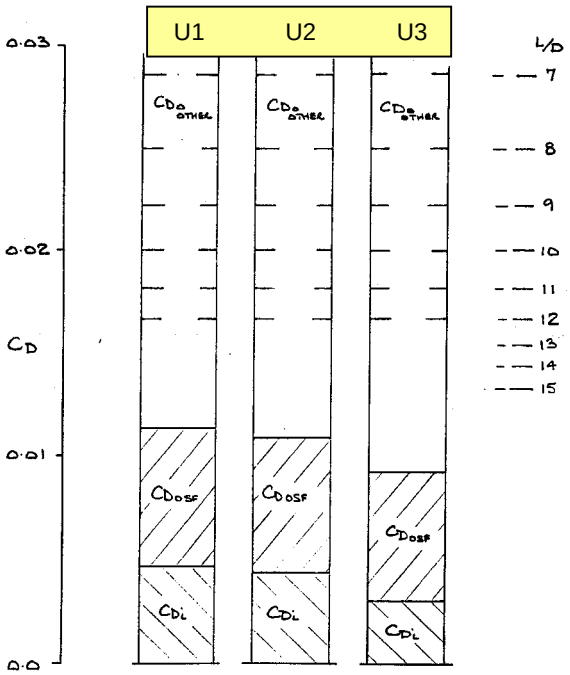


FIG. 31 PLANFORMS U1, U2 & U3, TOTAL DRAG BREAKDOWN,
$C_{Di}$ & $C_{Do}$ Contributions for Varying L/D at Mach 0.8, $C_L$ = 0.2

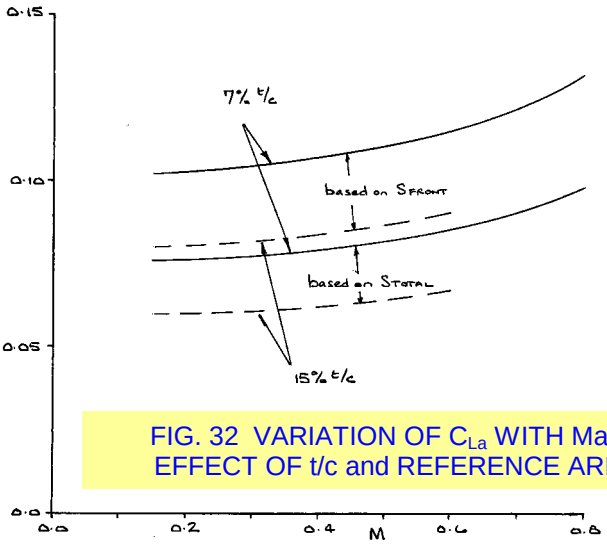


FIG. 32 VARIATION OF $C_{La}$ WITH Mach, EFFECT OF t/c and REFERENCE AREA

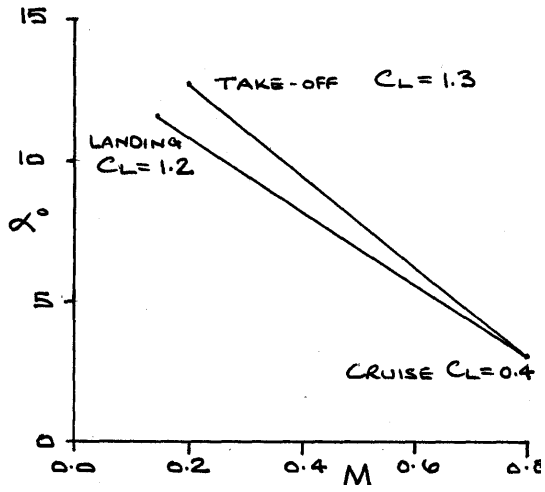


FIG. 33 INCIDENCE REQUIREMENTS AT TAKE-OFF, CRUISE and LANDING

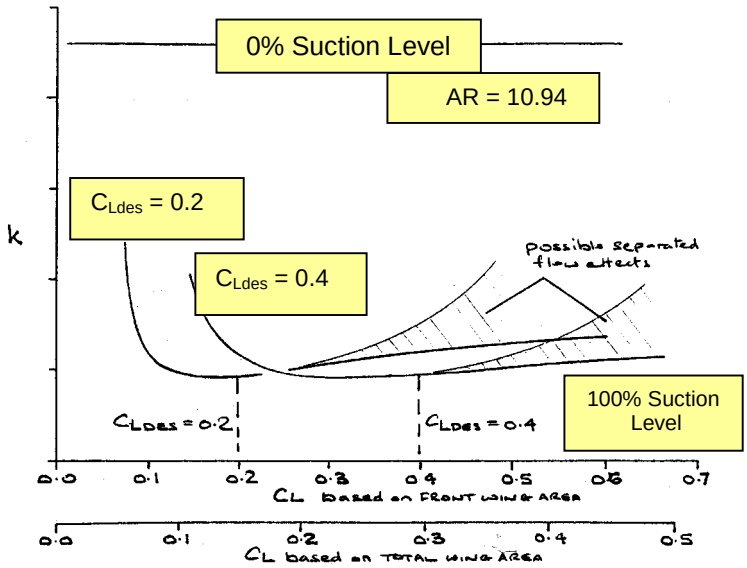


FIG. 34 VARIATION OF LIFT INDUCED DRAG FACTOR (k)

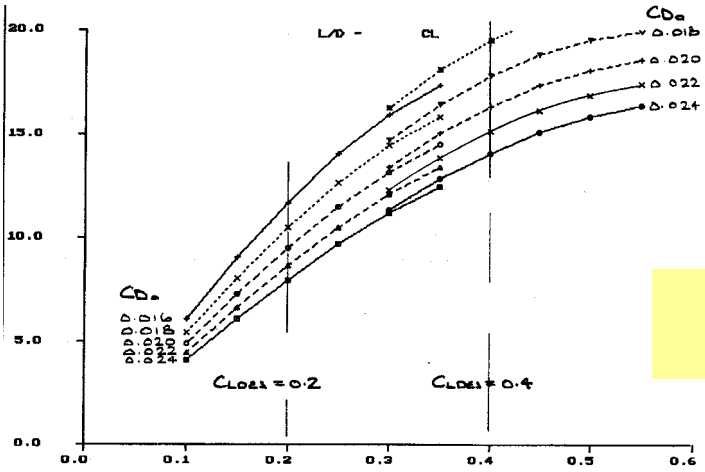


FIG. 36 L/D VARIATION WITH $C_L$ FOR A RANGE OF $C_{Do}$ VALUES, $C_{LDes}$ = 0.2 & 0.4, Mach 0.8

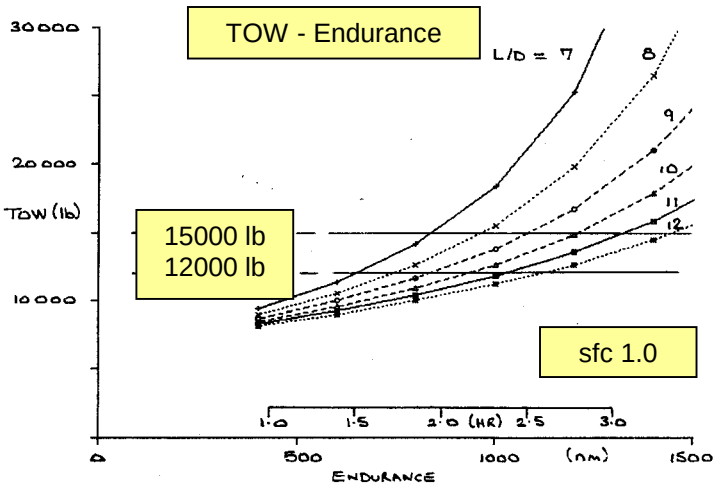


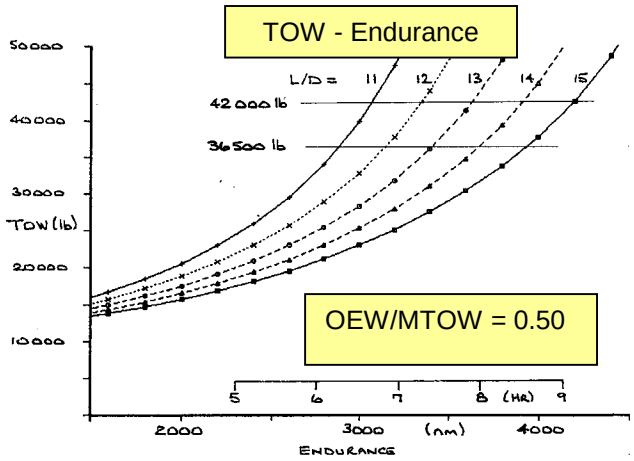


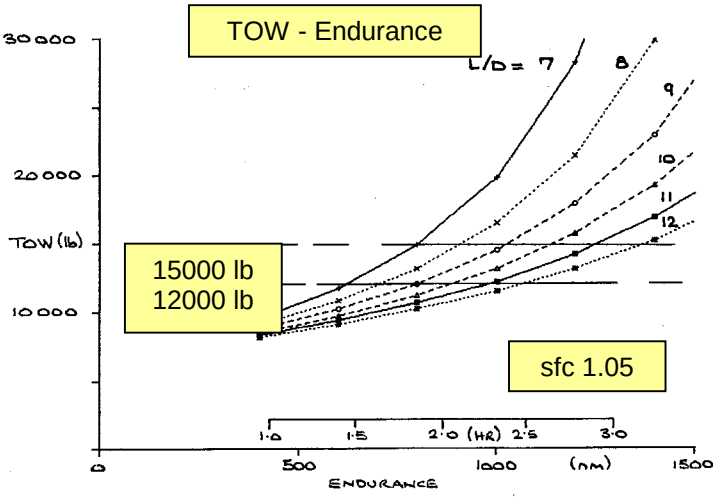


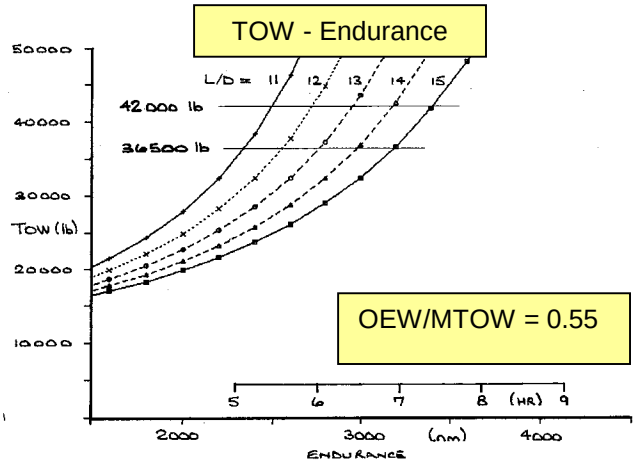


FIG. 37 U1, MTOW (lb) vs RANGE (nm), EFFECT OF L/D & sfc, Mach 0.75, OEW/TOW=0.55
(Allow for Short Cruise segment)

FIG. 38 CONFIG. U2 & U3, TOW (lb) vs RANGE (nm), EFFECT OF L/D & OEW/TOW, Mach 0.8, sfc 0.85

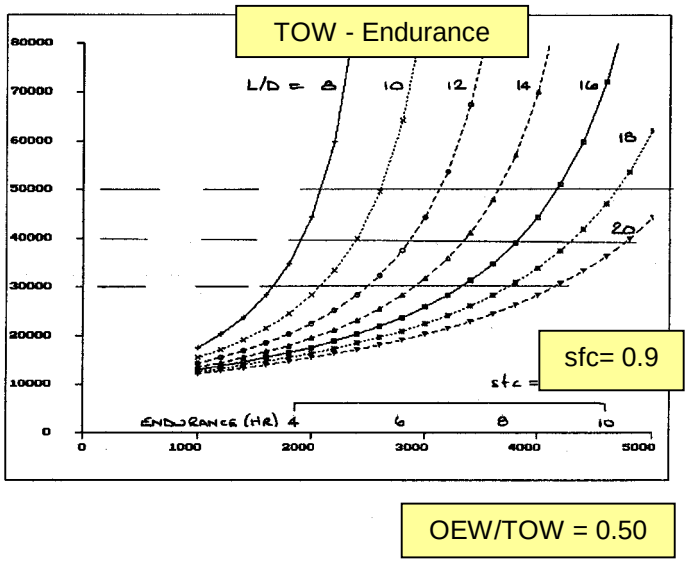


OEW/TOW = 0.50

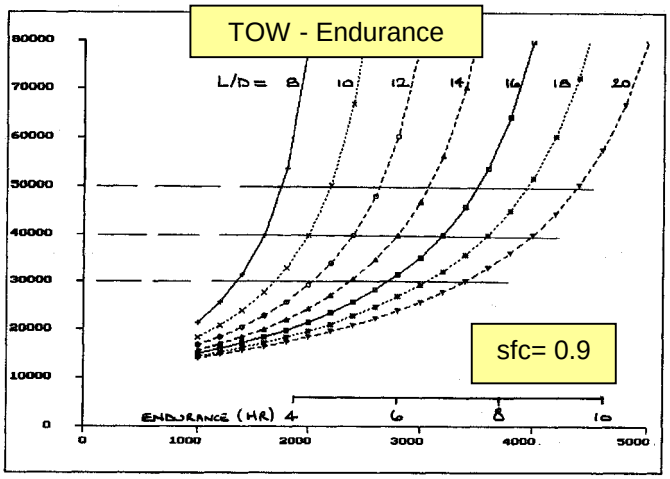


OEW/TOW = 0.55

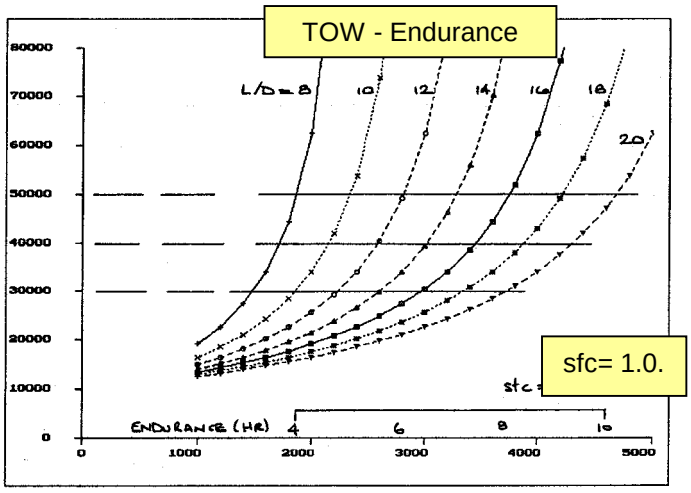


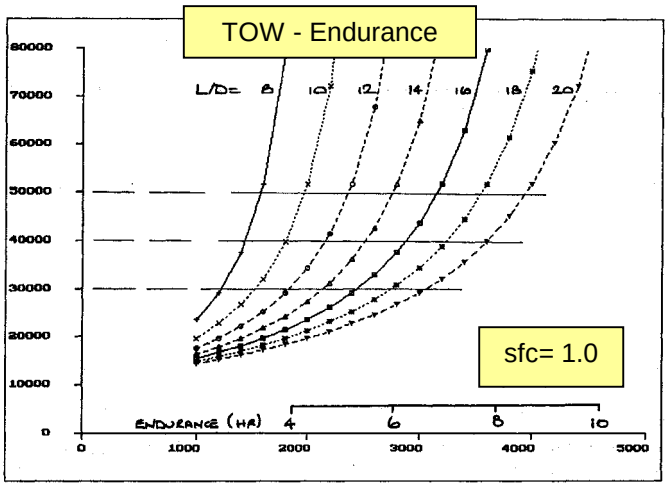


FIG. 39 TOW (lb) vs RANGE (nm) & ENDURANCE (hr), EFFECT OF L/D & sfc, OEW/TOW = 0.50, Mach 0.8

FIG. 40 TOW (lb) vs RANGE (nm) & ENDURANCE (hr), EFFECT OF L/D & sfc,

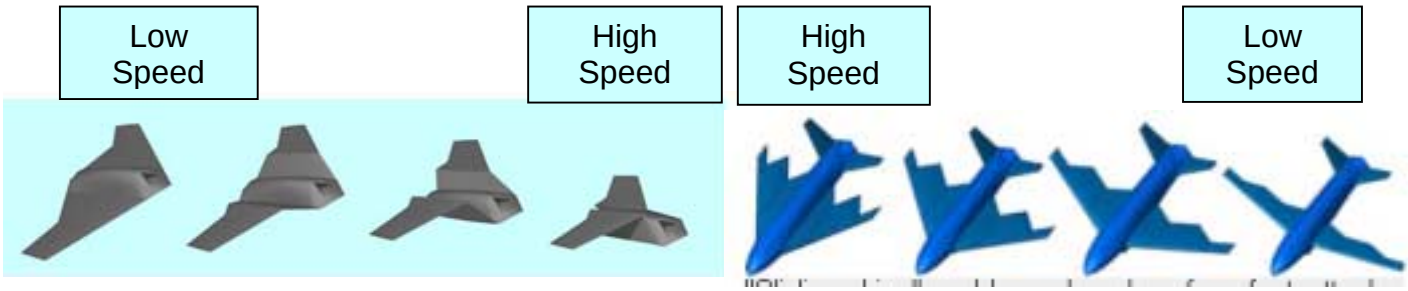


FIG. 41 FUTURE APPLICATIONS TO “MORPHING” WINGS